

AN EVALUATION OF THE APPLICABILITY OF PSEUDOSPECTRAL METHODS
TO PROBLEMS IN TRANSPORT PHENOMENA

by

GROVER TRAVIS JONES

B. S. Kansas State University, 1984

A MASTER'S THESIS

submitted in partial fulfillment of the

requirements for the degree

MASTER OF SCIENCE

Department of Chemical Engineering

KANSAS STATE UNIVERSITY
Manhattan, Kansas

1986

Approved by:


Major Professor

LD
2068
T4
1986
T66
c. 2

ALL206 737541

ABSTRACT

The objective of this work was the evaluation of pseudospectral methods for their computational efficiency and applicability to problems in transport phenomena. This was accomplished by application of Chebyshev pseudospectral methods to problems from each major area of transport phenomena. The evaluation of the pseudospectral method was based upon comparison to the analytic solution, if available, or finite difference approximation otherwise. It was found that discontinuities in the solution domain can result in serious deviations from the correct solution; for example, the temperature discontinuity in thermal entrance length problems led to the propagation of error within the solution. Digital filtering was used successfully to damp out oscillatory behavior in all cases studied.

ACKNOWLEDGEMENTS

I wish to express my gratitude to Dr. L. A. Glasgow for his patience, encouragement, and advise throughout my studies. I also wish to thank Mrs. Janet Vinduska who typed my thesis.

I wish to thank my father, Dr. W. Grover Jones for his constant support and encouragement throughout the time I have been at Kansas State University.

This work was partially supported by Air Force Grant SCEE-84-RIP-

TABLE OF CONTENTS

	Page
ACKNOWLEDGEMENTS	ii
TABLE OF CONTENTS	iii
LIST OF FIGURES	iv
LIST OF TABLES	v
 Chapter	
I. INTRODUCTION	1
II. REVIEW OF LITERATURE	5
III. APPLICATION OF THE CHEBYSHEV PSEUDOSPECTRAL METHOD	19
Start-up Laminar Velocity Profile	25
Transient Temperature Profile of a Wire Filament Electrically Heated	29
The Classical Graetz Problem	32
Diffusion in a Planar Slab	36
Diffusion and Reaction in Spherical Pellet	43
External Separated Flows	47
IV. CONCLUSIONS	55
APPENDIX A: STREAMLINE EXPRESSION FOR A PITCHED FLAT PLATE	57
APPENDIX B: COMPUTER PROGRAMS	59
LITERATURE CITED	74

LIST OF ILLUSTRATIONS

	Page
1. Temperature Profile within an Electrically Heated Wire Filament Obtained with Finite Difference and Pseudospectral Methods for $t=0.04$ seconds	31
2. Solutions to the Classical Graetz Problem from the Analytic Series Summation and the Pseudospectral method for $x/r_w = 0.075$	35
3. Ethanol Concentration Profiles within a Slab Obtained by a Finite Difference Representation and Pseudospectral Representations of 17,25, and 33 Terms, for $t=1000$ seconds.	39
4. Ethanol Concentration Profiles within a Slab Obtained by a Finite Difference Representation and Pseudospectral Representations of 17,25, and 33 Terms for $t=5000$ seconds	40

LIST OF TABLES

	Page
1. Comparison of pseudospectral predicted unsteady laminar flow to the analytical solution with four terms of the series being retained, $\tau = 0.05$	27
2. Comparison of pseudospectral and finite difference difference predicted flow to the analytical solution with four terms of the series being retained $\tau = 0.10$	28
3. Comparison of ethanol mole fractions at various points within a slab at a time of 1000 seconds for finite difference (FD) and pseudospectral methods.	41
4. Comparison of ethanol mole fractions at various points within a slab at a time of 5000 seconds for finite difference (FD) and pseudospectral methods.	42
5. Concentration profile within a spherical pellet at $\tau = 0.025$ determined by finite difference (FD) and pseudospectral approximations using filtering schemes I and II.	45
6. A comparison of concentration profiles within a spherical pellet after seven time increments for no filtering and filtering schemes I and II.	46
7. Comparisons of the first derivative of the Falkner-Skan equation for a 4th order Runge-Kutta method and Chebyshev collocation where N represents the number of terms retained in the series expansion.	50
8. Comparisons of the second derivative of the Falkner-Skan equation for a 4th order Runge-Kutta method and Chebyshev collocation where N represents the number of terms retained in the series expansion.	51

CHAPTER I. INTRODUCTION

Transport phenomena are pervasive in chemical engineering and accurate numerical solutions are requisite for improvements in process design and analysis. However, the evaluation of these equations is often difficult due to coupling and nonlinearity. This has given rise to many of the empirical relations used by practicing engineers today, and is largely responsible for the development of the "unit operations" approach. While empirical relations can be used for process design it is sometimes difficult to predict exactly what will happen if a particular variable is changed. With the universal availability of computers many, if not most, linear systems are now modeled numerically, allowing optimum operating characteristics to be determined.

The most popular numerical scheme for solving partial differential equations is the finite difference method which is easily applied to many problems. Finite difference techniques can be used in conjunction with explicit, implicit or hybrid methods depending upon the nature of the equation. Another popular numerical approach is the finite element method (see Finlayson [1980]). While a great amount of numerical work is carried out in all fields of Chemical Engineering some of the most advanced work has occurred in the area of fluid flow, primarily because of the nature of the Navier-Stokes equation, and the problem of turbulence. Consider the equations:

$$\frac{\partial u_i}{\partial t} + u_j \frac{\partial u_i}{\partial x_j} = \frac{1}{\rho} \frac{\partial p}{\partial x_i} + \nu \frac{\partial^2 u_i}{\partial x_j^2} \quad (1)$$

and

$$\frac{\partial u_i}{\partial x_i} = 0 \quad (2)$$

where u_i is the instantaneous velocity. This problem is often attacked using Reynolds decomposition by letting $u = U + u'$; where U is the mean velocity and u' is the fluctuation about the mean. The resulting equations are time averaged and simplified by noting that the linear terms in the fluctuating quantities are zero for a statistically stationary process. The result of this procedure is the Reynolds momentum equation:

$$\frac{\partial U_i}{\partial t} + U_j \frac{\partial U_i}{\partial x_j} = -\frac{1}{\rho} \frac{\partial p}{\partial x_j} + \frac{1}{\rho} \frac{\partial}{\partial x_j} \left(\mu \frac{\partial U_i}{\partial x_j} - \rho u'_i u'_j \right) \quad (3)$$

It is the introduction of $-\rho u'_i u'_j$ terms that constitutes the major difficulty confronting any analyst wishing to employ this method of attack upon the problem. An approximation for the turbulent momentum flux ($-\rho u'_i u'_j$) is necessary for calculation of many flows of interest. This term is usually related to mean flow velocity gradients multiplied by a proportionality function, or eddy viscosity. The result is in essence an empirical curve fitting approach in which constants are adjusted until the calculated and experimental results agree. Extrapolation from these results can be dangerous. It has been noted by many fluid dynamicists, including Tennekes and Lumley [1972] that gradient transport models are not appropriate for turbulent flow with multiple length or velocity scales.

There are alternatives to the Reynolds equation-turbulence modeling approach; these include sub-grid scale closure models and direct

numerical simulation of the Navier-Stokes equations. Deardorff [1970] has been the principal proponent of sub-grid scale closure--in this method, the large scale motions are explicitly obtained from the Navier-Stokes equations. The very small scale motions are treated statistically and in this manner the Reynolds number limitations of a total numerical simulation are avoided. Orszag [1977], among others, speaks in favor of this approach, while noting that the methods presently being used to handle the dissipative eddies are less than satisfactory. One would anticipate great difficulty in the direct simulation of the Navier-Stokes equation, since in the past 150 years, only about 75 analytic solutions have been found--a tribute to the intractability of simultaneous nonlinear partial differential equations. The pursuit of numerical solutions to the full set of equations is hindered by the rapid increases in degrees of freedom (nodal points in finite difference methods) with Reynolds number. Schumann et al. [1980], Liepmann [1979], and Orszag [1977] have all noted that the required degrees of freedom scale with $Re^{9/4}$. If it were possible to deal with a flow where $Re=100$ with 1000 interior mesh points, the scaling law suggests that $Re=10^4$ would require about 3×10^7 mesh points. In fact, Orszag notes that an order of magnitude increase in computational power will permit an increase in Re of only 2.15 times and Schumann et al. note that a brute-force simulation on a 10 MIPS machine for $Re=10^4$ would require about 3 years computing time. There are grounds for optimism, however, for free flows and flows in decay, where

either the Re is small or the large scale motions can be treated independently of the dissipative structure. There is less reason to be optimistic about success in direct simulation of flows about objects; for turbulent boundary layers or laminar boundary layers undergoing transition, the rapid changes in the streamwise direction cause difficulties in resolution. Furthermore, the downstream or outflow boundary conditions would appear to require complete specification in the wake region--with the concomitant danger that the flow will be over-specified and the results of the direct simulation set in advance.

Therefore, there is need for numerical methods in which there is not a rapid increase in the degrees of freedom with increasing Reynolds number for the full set of Navier-Stokes equations and which also does not require "numerical" boundary conditions in addition to those specified by the original problem. Preferably, it should be possible to apply this approach easily to any problem of interest.

CHAPTER II

REVIEW OF LITERATURE

For the above reasons the decision was made to explore the spectral methods described in the monograph of Gottlieb and Orszag [1977] and the review of Gottlieb et al [1984a]. Spectral methods have become increasingly popular in recent years resulting in studies of transitional fluid flows (Kleiser [1982], Marcus et al. [1982] and Orszag and Kells [1980]); incompressible fluid flow simulations (Haidvogel et al. [1980], Kumar and Yajnik [1980], Leonard and Wrey [1982], Moin [1982], Moin and Kim [1980], Orszag [1971, 1980] and Taylor and Murdock [1980,1981]); and most recently for complicated compressible flow fields which include shock waves (Gottlieb et al. [1981, 1984b], Hussaini and Zang [1984], Sakell [1984] and Salas et al. [1982]). Interest in spectral methods is due in part to the increased accuracy available for a given number of independent degrees of freedom (i.e. the number of mesh nodes for a finite difference method) in comparison to finite difference techniques; for example see Haidvogel et al. [1980] or Dennis and Quartapelle [1982] for comparisons of accuracy. The spectral methods are often referred to as being infinite-order accurate, that is, if after N terms the error decreases more rapidly than any power of $1/N$. Orszag [1971] states that it is possible to decrease the computational time and storage by an order of magnitude. The advent of the fast Fourier transform in the mid 60's facilitated the development of spectral methods, since rapid evaluation of trigometric polynomial coefficients became possible. Much of the work done with respect to fluid dynamics has involved the use of

the pseudospectral techniques also known as "collocation" or the "method of selected points" (Lanczos [1956]).

Spectral methods represent the solution to the problem as a truncated series of eigenfunctions for the independent variable. The type of series expansion used is based upon the type of boundary condition that is to be satisfied, for example, a periodic boundary condition would suggest the use of a Fourier series representation for the solution. Gottlieb and Orszag [1977] and Orszag [1977] suggest the following series representations:

<u>Boundary Conditions</u>	<u>Series Representation</u>
periodic	$\exp(inx)$
inviscid	$\sin(nx)$ or $\cos(nx)$
no-slip	Chebyshev ($T_n(x)$) or Legendre ($P_n(x)$)

The most popular series representations are the sine series and the Chebyshev series due in part of the ability to use the FFT to evaluate coefficients or their inverse transform. Additional series representations have been used for special problems; for example Tang [1979] used surface harmonics as the expansion function for two dimensional flows on the surface of a sphere and Kasahara [1977] used Hough harmonics to solve shallow-water equations over a sphere. Typically the series representation was an eigenfunction expansion for the governing equation. Gottlieb and Orszag [1977] discuss the convergence properties of various series expansions and conclude that for "non-slip" boundary conditions that Chebyshev or Legendre series provide the greatest accuracy for the fewest terms in the expansion.

Spectral methods can be classified as Galerkin, Tau, or Pseudospectral. A Galerkin method seeks the approximation of the dependent variable, $u_N(x,t)$, in the form of a truncated series.

$$u_N(x,t) = \sum_{n=1}^N a_n(t) \phi_n(x) \quad (4)$$

where $\phi_n(x)$ are linearly independent functions chosen such that $u_N(x,t)$ satisfies all boundary conditions. The coefficients, $a_n(t)$, are determined by the Galerkin equations:

$$\frac{d}{dt} \int_D \phi_n x \phi_n u_N dx = \int_D \phi_n L u_N dx + \int_D \phi_n f dx \quad (n = 1, 2, \dots, N) \quad (5)$$

where L is a linear differential operator. The tau method developed by Lanczos [1956] employs expansion functions, ϕ_n , assumed to be elements of a complete set of orthonormal functions. The approximation to the solution, $u_N(x,t)$ is expressed

$$u_N(x,t) = \sum_{n=1}^{N+k} a_n(t) \phi_n(x) \quad (6)$$

where k is the number of independent boundary constraints that must be applied. The coefficients a_{N+1} to a_{N+k} are chosen such that the k boundary conditions are satisfied. Whereas the expansion coefficients a_1 to a_N are the approximate solutions for the differential equation being solved. Collocation methods represent the solution, u_N , as a series expansion:

$$u_N = \sum_{n=1}^N a_n \phi_n(x) \quad (7)$$

where the expansion coefficients a_n are the solutions of the equations

$$\sum a_n \phi_n(x_i) = u(x_i) \quad (8)$$

Notice that the coefficients a_n are dependent on both ϕ_n and the points x_n for $n=1, 2, \dots, N$. Collocation methods can be applied in either normal or spectral space (i.e. solve for u_n or a_n , respectively) but, most often are applied in normal space because of the nonlinear nature of the governing equation. The greatest difference between these methods is the manner in which boundary conditions are handled (see section 2 of Gottlieb and Orszag [1977]).

Pseudospectral (collocation) techniques are the most likely to be appropriate for typical governing equations of transport phenomena. The principal concept behind pseudospectral calculations as stated by Orszag [1980] is to simply transform freely between physical (x_j) and spectral (a_n) representations, evaluating each term in whatever representation that term is most accurately, and simply evaluated. Pseudospectral computations have several advantages over spectral algorithms: 1) For complex geometry the solution of the spectral (Galerkin) method requires at least twice the number of fast Fourier transforms than that of the pseudospectral method using trigometric series representation; 2) Pseudospectral techniques have significant advantages over spectral techniques when solving nonlinear partial differential equations especially when considering computational expense.

In order to demonstrate the spectral method consider the one dimensional transient equation:

$$\frac{\partial u}{\partial t} = \frac{\partial^2 u}{\partial x^2} \quad (9)$$

with the boundary and initial conditions

$$\begin{aligned} u(0,t) &= u(\pi,t) = 0 \\ u(x,0) &= f(x) \end{aligned} \quad (10)$$

the analytic solution to this problem can be shown to be

$$u(x,t) = \sum_{n=1}^{\infty} \left\{ \frac{2}{\pi} \int_0^{\pi} f(x) \sin(nx) dx \right\} \sin(nx) \exp(-n^2 t) \quad (11)$$

Therefore, let u_N be the spectral approximation to u , so that the solution can be approximated as

$$u_N(x,t) = \sum_{n=1}^N a_n(t) \sin(nx) \quad (12)$$

Substituting back into equation (12) and using the Fourier transform results in

$$\frac{da_n(t)}{dt} = -n^2 a_n(t) \quad (13)$$

and this set of ordinary differential equations is solved with respect

to the initial conditions $a_n(0) = \frac{2}{\pi} \int_0^{\pi} f(x) \sin(nx) dx$ ($n=1, \dots, N$).

Gottlieb and Orszag [1977] have shown for this example that $u(x,t) - u_N$

(x,t) goes to zero more rapidly than $\exp(-N^2 t)$ for any $t > 0$ and $N \rightarrow \infty$.

It can be seen that the spectral approximation of $u(x,t)$ that results is a truncation of the exact solution to N terms. In contrast to this

exceedingly good approximation it is possible to construct a spectral method that will arrive at extremely poor results; therefore care must be exercised in the construction of a spectral approximation.

The pseudospectral method is typically chosen over other spectral methods when considering a nonlinear equation. For example consider

$$\frac{\partial u}{\partial t} = \exp(xu) \frac{\partial u}{\partial x} + \frac{\partial^2 u}{\partial x^2} \quad (14)$$

let the approximation $u_N(x, t)$ to $u(x, t)$ be

$$u_N(x, t) = \sum_{n=1}^N a_n(t) \psi_n(x) \quad (15)$$

where $\psi_n(x)$ is an orthonormal function. Then the spectral approximation will be

$$\frac{da_n(t)}{dt} = \int \psi_n \left\{ \exp[x \sum a_n \psi_n] \sum a_n \psi_n' + \sum a_n \psi_n'' \right\} dx \quad (16)$$

It is seen that these equations for $a_n(t)$ are computationally complex due to the resulting integro-differential equation for $a_n(t)$. Therefore, consider the pseudospectral method in which, N collocation points (x_1, x_2, \dots, x_N) lying within the computational domain are introduced. The approximation (15) is forced to satisfy the governing partial differential equation (14). For example, the following steps would be followed; 1) Determine N coefficients $a_n(0)$ such that

$$u_N(x_j, 0) = \sum_{n=1}^N a_n(0) \psi_n(x_j) \quad (17)$$

2) Evaluate each term of the governing partial differential equation in either physical or spectral space, whichever gives the most accurate and easily obtainable approximation. For example, $\exp(x_j u_N(x_j, t))$ is evaluated in physical space since the value for $u_N(x_j, t)$ is known and the partial derivatives are evaluated in spectral space since this results in the most accurate representation. 3) Integrate in time with respect to $u_N(x_j, t)$ using the "leap-frog" method or another suitable choice. 4) Repeat steps 1)-3) until the time integration is completed. From this example pseudospectral methods are seen to be much easier to apply to nonlinear equations than corresponding spectral techniques.

The application of boundary conditions in a spectral method can determine the solution's stability. Gottlieb et al. [1981] state that incorrect boundary treatments may give strong instabilities in contrast to finite-difference methods in which this would appear as relatively weak oscillations. Moin and Kim [1980] note that fully explicit pseudo-spectral solution of the incompressible Navier-Stokes equation have an inherent numerical problem for viscous flows involving solid boundaries, due to enforcing no-slip conditions at the walls. Rudy and Strikwerda [1981] presented a study of inflow and outflow boundary conditions for compressible Navier-Stokes equations of flow past a flat plate. This study, conducted for finite-difference methods of solution, indicates that errors in the data specified at the inflow boundary condition can significantly affect the solution obtained. Gottlieb and Orszag [1977] note spectral methods are extremely sensitive to the formulation of

boundary conditions; for example, when improper boundary conditions are imposed, the solution is likely to be "explosively" unstable.

Convergence of the spectral (Galerkin) method for Navier-Stokes equations has been demonstrated for a Fourier representation with periodic boundary conditions by Hald [1981]. Maday and Quarteroni [1982] have provided stability results and "optimal" convergence rates for Galerkin and pseudospectral approximations (using trigonometric polynomials) for the stationary Navier-Stokes equation with periodic boundary conditions. Canuto [1984] analyzed explicit and implicit methods of imposing boundary conditions for Chebyshev and Legendre approximations of elliptic problems ensuring stability and convergence for these methods. Canuto and Quarteroni [1984] give stability and "optimal" convergence rates for Chebyshev collocation approximations of variable coefficient elliptic problems with Dirichlet or Neumann-type boundary conditions. Gottlieb [1981b] has demonstrated stability of Chebyshev-pseudospectral representations for parabolic and hyperbolic equations with variable coefficients. Gottlieb and Orszag [1977] discuss algebraic stability criteria as applied to spectral methods. Pasciak [1980] investigated spectral and pseudospectral representations of advection equations with the intention of introducing a framework in which finite elements analysis can be applied to spectral methods. In addition error estimates are given for fully discrete explicit pseudospectral as well as semidiscrete spectral and pseudospectral methods.

Some additional considerations warrant attention. In the case of a discontinuity, the rate of convergence in the region of the discontinuity is seriously degraded, but spectral approximations are still

normally more accurate than corresponding finite difference representations (Gottlieb and Orszag [1977]). Additionally, the error is localized better by the spectral method such that less local dissipation is required to smooth the discontinuities. If dissipation or a filtering technique is not used then Gibb's phenomenon is seen in the region of the discontinuity, and, the resulting error from the lack of smoothing pollutes the solution globally (Osher [1984]). Majda et al. [1978] have shown for general linear hyperbolic Cauchy problems with nonsmooth initial data that the appropriate smoothing techniques applied to the equation results in stability and that this smoothing combined with smoothing of the initial data gives rise to infinite order accuracy away from the discontinuities of the exact solution. The most prominent examples of discontinuities that have been examined by spectral methods are shock waves (Gottlieb et al. [1981,1984b], Hussaini and Zang [1984], Sakell [1984], Salas [1982], Streett et al. [1985], and Taylor et al. [1981]). A variety of filters and dissipation functions have been used to damp the oscillations occurring in the solution due to the discontinuity. For example, one sided Schumann filter (Gottlieb et al. [1981]), von Hann window filter (Hussaini and Zang [1984] and Salas [1982]), second and fourth-order artificial viscosity (Sakell [1984] and Streett et al. [1985]), artificial density (Street et al. [1985]) as well as the method of Boris and Book [1976], originally developed for the construction of finite difference algorithms involving strong shocks (Taylor et al. [1981]), have produced accurate, smooth solutions for this type of problem. In addition, Gottlieb et al. [1981] used a low-pass spectral filter to remove the high frequency waves that lead to

instability and a "cosmetic" filter (a one-sided Schumann filter) to find a nonoscillatory numerical solution. Gottlieb [1985] provides a brief review of recent advancements in the field of compressible flow problems. Streett and Bradley [1985] discuss briefly some applications of spectral methods in aerodynamics.

Symmetric flow past a flat plate has been treated by Orszag [1971] and Taylor and Murdock [1980],[1981]. Planar flow has been investigated by Moin and Kim [1980], Orszag and Kells [1980] and Kleiser [1982]. Taylor and Murdock studied the flow over a flat plate in a range of $1.2 \times 10^5 < Re < 3.8 \times 10^5$, which is well within the turbulent flow regime. The velocity profile was solved as perturbation about the Blasius velocity profile. Taylor and Murdock used a mesh of 17×17 to solve for the velocity profile, while Orszag used nine collocation points to approximate a one dimensional boundary layer, both studies resulted in accurate approximations.

The treatments of transonic flow by Gottlieb et al. [1984b] and Streett et al. [1985] are interesting in that spectral methods (Chebyshev collocation) are being used. The treatment of transonic flow over an airfoil can be viewed as state-of-the-art application of spectral methods because of the difficulty posed by the sharp shock gradients and the computational competition with finite difference methods. Again, it is seen that separation causes difficulty as Streett et al. note that the potential equation which is being solved becomes a mixed elliptic-hyperbolic type and admits weak solutions with

discontinuities. Streett et al. use artificial viscosity with a directional bias introduced in the potential equation in the supersonic region to suppress the appearance of compression and expansion shocks due to the presence of a supersonic bubble. It is apparent that the use of multigrid techniques has made spectral methods for steady compressible flow competitive with finite difference methods for problems of aerodynamic interest.

A very thorough review of application and major developments of spectral methods from approximately 1977 to 1983 is provided by Gottlieb et al. [1984a]. This review presents all major aspects of applying spectral methods to Navier-Stokes equations. Taylor et al. [1985] have proposed a method for solving the primitive three dimensional (3-D) Navier-Stokes equations without introducing the Poisson equation for pressure. This was accomplished by integrating the equation of continuity for the normal velocity component with respect to the surface and integrating the corresponding equation of motion to evaluate the pressure term. This procedure, applied to evaluate boundary layer stability, was found to be the same as a marching solution of a Poisson equation and therefore unstable. A second method was proposed in which the normal velocity component was evaluated from both the equation of continuity (V_c) and the equation of motion (V_m) and an iterative method of the following form:

$$p^{n+1} = p^n + \alpha \frac{\partial}{\partial y} (V_c - V_m) \quad (18)$$

was used to evaluate the pressure at the new time. They found this approach to converge very slowly due to its explicit nature. Malik et

a1. [1985] describe a Fourier-Chebyshev spectral method for the incompressible Navier-Stokes equations. The algorithm, combines a fully spectral scheme with a Fourier-finite difference method in evaluating most wall bounded shear flows. Zang and Hussaini [1985] have employed this algorithm, with appropriate modifications, using Fourier-Legendre expansions to model incompressible channel flow. Satisfactory results were obtained. It should be noted that while Legendre series and Chebyshev series require approximately the same number of terms to converge to the solution, (Gottlieb and Orszag [1977]) Legendre series are rarely used in practice. While the FFT is much faster than matrix inversion for large matrices as the matrix size decreases the efficiency of the FFT also decreases until it is approximately that of matrix inversion; therefore Legendre representations should be competitive Chebyshev representations when "few" terms are required for an accurate approximation. Taylor [1984] has shown that for $N < 64$ that Crout's method is equivalent or better than the FFT. Also Zang and Hussaini note that evaluation of derivatives by matrix multiplication (Legendre collocation matrices) is faster for $N=32$ than machine language Chebyshev transforms.

Many methods are being used to solve spectral representations, for example, Deville et al. [1982] examined time integration for the non-linear Burger equation. They conclude that only two methods are practical choices: The first employs a second order Adams-Bashforth method to integrate the non-linear terms and a second order Crank-Nicolson scheme to integrate the linear terms and the second method utilizes predictor and corrector steps and both finite difference and

pseudospectral methods. Taylor [1984] outlines a finite difference predictor and spectral corrector approach for integration. An ADI method has been used to solve a Poisson equation (Haidvogel and Zang [1979]). Haidvogel and Zang described a second algorithm for Poisson's equation in which the tau method is used and the resulting coefficient matrix for the second order derivative is diagonalized. This approach is better suited to time-dependent problems and is an order of magnitude more efficient than the ADI algorithm. Haldenwang et al. [1984] have used this algorithm for a 3-D Helmholtz equation. The use of non-homogeneous boundary conditions with the resulting equations for evaluation of derivatives is discussed in Appendix I of the Haldenwang et al paper. Sharp and Harris [1984] have investigated the combination of pseudospectral methods with parametric differentiation as applied to the Falkner-Sakan equation. From CPU times given for evaluation of the equation, it does not appear that the method of parametric differentiation combined with a pseudospectral expansion is competitive with the pseudospectral method. Zebib [1983] has proposed a new Chebyshev method which represents the highest derivative as a Chebyshev series expansion with lower derivatives being obtained by integration. This technique can be viewed as being related to the tau method in that additional terms arising from the integration are used to satisfy boundary conditions. From the examples presented the method appears to be fully as accurate as more traditional Chebyshev techniques.

For cases where fully spectral techniques are difficult to apply or inappropriate for the problem domain other avenues are available for their application. One possible method is the combination of finite

difference and pseudospectral methods for separate directions. Reddy [1983] used such an approach in solving 3-D flowfields over missile shaped configurations at moderate angles of attack. In this approach a Fourier sine series was used in the circumferential direction with finite difference representation for the other directions. Reddy estimated that a 40% increase in efficiency could be obtained for a relatively sparse grid with respect to the spectral representation. Metivet and Morchoisne [1982] have investigated splitting the domain on which the problem is defined into a finite number of problems on subdomains. Metivet and Morchoisne note the main considerations of this approach are "patching" (i.e. ensuring that derivatives at the boundaries of adjacent subdomains are continuous) and modifications of equations due to mapping of the subdomains. The proposed method has the flexibility of finite element and finite difference methods, but maintains the accuracy of monodomain spectral techniques.

It is evident that spectral methods can be applied competitively to many aerodynamic and hydrodynamic flow simulations. Since equations for heat and mass transfer are often similar to those of fluid flow, it is likely that spectral methods can be applied profitably in those cases as well. The purpose of this work is to investigate the application of spectral methods to problems in transport phenomena and to assess the suitability and computational efficiency of such methods when applied to important nonlinear equations.

CHAPTER III. APPLICATION OF THE CHEBYSHEV PSEUDOSPECTRAL METHOD

In order to discuss how Chebyshev collocation is applied, it is advantageous to have a framework for the evaluation of coefficients and derivatives. A Chebyshev series is defined on the interval $(-1,1)$ with the interpolation points most commonly chosen as

$$x_j = \cos \frac{\pi j}{N} \quad (j = 0, 1, \dots, N) \quad (19)$$

for a N th-order representation. A Chebyshev polynomial of degree n is defined

$$T_n(x) = \cos(n \cos^{-1}(x))$$

therefore it follows

$$T_n(x_j) = \cos \frac{\pi j n}{N} \quad (j = n = 0, 1, \dots, N) \quad (20)$$

Based on these definitions the approximation to the solution $U_N(x_j)$

is:

$$\begin{aligned} U_N(x_j) &= \sum_{n=0}^N a_n T_n(x_j) \\ &= \sum_{n=0}^N a_n \cos \frac{\pi j n}{N} \end{aligned} \quad (21)$$

where a_n are the polynomial coefficients. The coefficients are evaluated by application of a Fourier transform resulting in:

$$c_n a_n = \frac{2}{N} \sum_{j=0}^N c_j^{-1} U_N(x_j) \cos \frac{\pi j n}{N} \quad (n=0, 1, \dots, N) \quad (22)$$

where $c_0 = c_N = 2$ and $c_j = 1$ for $0 < j < N$. This transform can be expressed in terms of matrices

$$a = T^s U_N \quad (23)$$

where

$$a = \begin{bmatrix} a_0 \\ a_1 \\ \vdots \\ a_N \end{bmatrix}, \quad U_N = \begin{bmatrix} U_N(x_0) \\ U_N(x_1) \\ \vdots \\ U_N(x_N) \end{bmatrix}$$

and

$$T^s = \frac{2}{N} \begin{bmatrix} \frac{T_0(x_0)}{4} & \frac{T_0(x_1)}{2} & \frac{T_0(x_2)}{2} & \dots & \frac{T_0(x_N)}{4} \\ \frac{T_1(x_0)}{2} & T_1(x_1) & T_1(x_2) & \dots & \frac{T_1(x_N)}{2} \\ \frac{T_2(x_0)}{2} & T_2(x_1) & T_2(x_2) & \dots & \frac{T_2(x_N)}{2} \\ \vdots & \vdots & \vdots & \dots & \vdots \\ \frac{T_N(x_0)}{4} & \frac{T_N(x_1)}{2} & \frac{T_N(x_2)}{2} & \dots & \frac{T_N(x_N)}{4} \end{bmatrix}$$

Now consider the derivative of U_N which can be expressed in terms of polynomial series the following manner

$$\frac{d}{dx} \{U_N(x)\} = \sum_{n=0}^N a_n \frac{d}{dx} \{T_n(x)\}$$

for a Chebyshev representation this can be rewritten

$$\frac{d}{dx} \{U_N(x)\} = \sum_{n=0}^N b_n T_n(x) \quad (24)$$

where $b_N = 0$. The relation between the coefficients a_n and b_n can be shown to be

$$b_n = \frac{2}{c_n} \sum_{\substack{p=n+1 \\ p+n \text{ odd}}}^N p a_p \quad (25)$$

based on the recurrence property

$$2T_n'(x) = \frac{\tilde{c}_n T_{n+1}'(x)}{n+1} - \frac{w_n T_{n-1}'(x)}{n-1} \quad (26)$$

where $\tilde{c}_n = w_n = 0$ if $n < 0$, $\tilde{c}_0 = 2$, $w_0 = 1$, and $\tilde{c}_n = w_n = 1$ for $n > 0$, and the prime indicates differentiation. The coefficient representation for the second derivative can be shown to be:

$$d_n = \frac{1}{c_n} \sum_{\substack{p=n+2 \\ p+n \text{ even}}}^N p(p^2 - n^2) a_p \quad (27)$$

where

$$\frac{d^2}{dx^2} \{U_N\} = \sum_{n=0}^N d_n T_n(x) \quad (28)$$

and $d_N = d_{N-1} = 0$. The evaluation of derivative coefficients can be represented in matrix fashion. Consider the coefficients of the first derivative

$$b = D^{(1)} a \quad (29)$$

where

$$b = \begin{bmatrix} b_0 \\ b_1 \\ \vdots \\ b_N \end{bmatrix}$$

and

$$D_{ij}^{(1)} = 0 \text{ if } i > j \text{ or } i+j \text{ even}$$

otherwise

$$D_{ij}^{(1)} = \frac{2j}{c_i} \text{ for } i=j=0,1,\dots,N$$

The second derivative coefficients can be expressed

$$d = D^{(1)}b = [D^{(1)}D^{(1)}a] = D^{(2)}a \quad (30)$$

where

$$d = \begin{bmatrix} d_0 \\ d_1 \\ \vdots \\ d_N \end{bmatrix}$$

It can be seen that any order derivative can be evaluated by raising $D^{(1)}$ the appropriate power, q , where q is less than N . Ku and Hatzivramidis [1985] have taken this approach a step further by noting

$$\begin{aligned} \frac{d}{dx}(U_N) &= T^n D^{(1)} a \\ &= T^n D^{(1)} T^s U_N \end{aligned} \quad (31)$$

or for a q th order derivative

$$U_N^{(q)} = T^n (D^{(1)})^q T^s U_N \quad (32)$$

where

$$T^n = \begin{bmatrix} T_0(X_0) & T_1(X_0) & T_2(X_0) & \dots & T_N(X_0) \\ T_0(X_1) & T_1(X_1) & T_2(X_1) & \dots & T_N(X_1) \\ T_0(X_2) & T_1(X_2) & T_2(X_2) & \dots & T_N(X_2) \\ \vdots & \vdots & \vdots & & \vdots \\ \cdot & \cdot & \cdot & & \cdot \\ T_0(X_N) & T_1(X_N) & T_2(X_N) & \dots & T_N(X_N) \end{bmatrix}$$

They note that this procedure is as accurate as the FFT in evaluating derivatives and is more efficient in terms of computational time and implementation. The basic framework for evaluation of derivatives and coefficients has been established.

There are limitations to the above approach. One of the most notable exceptions is the application of Robin's boundary conditions at the interface of two calculated domains (i.e. flux equated across the boundary). Often the derivatives of the dependent variable for the first one or two points beyond the boundary are not very accurate in the pseudospectral representation due to aliasing. For a cosine function $\cos(\omega x)$, the frequencies ω and $-\omega$ are indistinguishable and are said to be aliases of each other. More specifically when a Fourier transform is used to transform a function into spectral space and back again the result is:

$$\hat{w}(k) = w(k) + w(k+2K) + w(k-2K) \quad (|k| < K) \quad (33)$$

where $\hat{w}(k)$ is the aliased representation of $w(k)$ and $N = 2K$. The last two terms arise from the fact that $\exp[i(k \pm N)x_j] = \exp[ikx_j]$ for all

integral j and k . It should be noted that for $|k| \ll K$ only one of the two terms due to aliasing can be non zero. Therefore, the values of the derivative at the boundary must be forced to satisfy the required condition. This can be accomplished either by direct substitution of the derivative value, if possible, or by the use of the tau method. Additional summation terms are needed for the cases where aliasing is significant and hence has to be removed. A matrix approach may be difficult to apply for the case of nonlinear problems. Therefore, in certain cases, it may be easier to eliminate the aliasing if the governing equation is represented in terms of the series coefficients. Another example is when a spectral filter is desired to eliminate "noise" from the solution arising from a discontinuity. Again, it is easier to use the series coefficients in a spectral filtering method than to use the dependent variable values.

Using the preceding approach classical problems in fluid and thermal transport and two additional problems dealing with diffusion were studied. The classical problems considered were; 1) Start-up laminar velocity profile in a circular tube; 2) Transient temperature profile of a wire filament electrically heated; 3) The classical Graetz problem. Diffusion in which diffusivity was a function of concentration was modeled for a planar geometry. The last problem considered was transient diffusion and reaction within a spherical pellet, with nonlinear Michaelis-Menton kinetics (typically seen for many enzymes).

Start-up Laminar Velocity Profile

The simplest problem considered is the start-up of the laminar velocity profile in a circular tube. This problem is considered simple because of the linearity of the governing equation, which is given by:

$$\rho \frac{\partial v}{\partial t} = \frac{p_0 - p_L}{L} + \mu \frac{1}{r} \frac{\partial}{\partial r} \left(r \frac{\partial v}{\partial r} \right) \quad (34)$$

v is the fluid velocity, ρ is the density of the fluid, t is time, $\frac{p_0 - p_L}{L}$ is the applied pressure gradient, μ is the fluid viscosity and r is the tube radius. The following initial (I.C.) and boundary conditions (B.C.'s) were used:

$$\text{I.C.} \quad v(r, 0) = 0; \quad 0 < r < R \quad (35)$$

$$\text{B.C.'s} \quad v(R, t) = 0; \quad t > 0 \quad (36)$$

$$\frac{\partial v}{\partial r} (0, t) = 0; \quad t > 0 \quad (37)$$

The analytic solution to this problem expressed in terms of the dimensionless variables ϕ , ξ and τ where

$$\phi = \frac{v}{(p_0 - p_L)R^2 / 4\mu L}; \quad \xi = \frac{r}{R}; \quad \tau = \frac{\mu t}{\rho R^2}$$

is

$$\phi(\xi, \tau) = (1 - \xi^2) - 8 \sum_{n=1}^{\infty} \frac{J_0(\alpha_n \xi) \exp[-\alpha_n^2 \tau]}{\alpha_n^3 J_1(\alpha_n)} \quad (38)$$

The α_n are chosen such that the resulting zeroth order Bessel function ($J_0(\alpha_n)$) is zero. The pseudospectral approximation, ϕ_N , to the solution, ϕ , was expressed by a Chebyshev polynomial expansion. The governing equation was integrated with an Euler predictor. Table 1

illustrates the results obtained for this problem with nine and seventeen expansion terms and $\tau = 0.05$. Table 2 illustrates the results obtained for this problem with seventeen and twenty-five expansion terms and $\tau = 0.10$, results for a finite difference representation are included.

Tables 1 and 2 illustrate that fairly accurate approximations are obtained for the central region of the tube. Table 2 indicates that no significant increase in accuracy is obtained by increasing the number of coefficients. An anomaly seen for the pseudospectral approximations is the relative inaccuracy of the solution near the boundary in relation to that of the central region. The cause of this inaccuracy may be due to the integration method chosen or presence of a discontinuity at the boundary when the pressure gradient is initiated. The results presented in Table 2 suggest the integration method used was relatively accurate and therefore the problem in the boundary region is due to the initial discontinuity. Possible methods to deal with the problem of the initial discontinuity include using a digital filter to remove any "noise" that may occur near the boundary, the use of a more accurate integration scheme, or use of a highly accurate finite difference representation to initialize the values of the pseudospectral approximation at some point beyond the initial starting values. Aliasing is not a factor in this case, since as Orszag [1972] has noted, aliasing terms lead to the numerical solution being susceptible to numerical instability.

Table 1. Comparison of pseudospectral predicted unsteady laminar flow to the analytical solution with four terms of the series being retained, $\tau = 0.05$.

	1.0	0.9239	ξ 0.7071	0.3827	0.0
$\phi(0.05, \xi)$	0.0	0.1054	0.2056	0.1941	0.2000
$\phi_8(0.05, \xi)$	0.0	0.07848	0.1796	0.1998	0.2032
% Error	0.0	25.5	112.6	3.0	1.6
$\phi_{16}(0.05, \xi)$	0.0	0.06040	0.1579	0.1959	0.1976
% Error	0.0	42.7	23.2	0.93	1.2

Table 2. Comparison of pseudospectral and finite difference predicted flow to the analytical solution with four terms of the series being retained, $\tau = 0.10$.

	ξ				
	1.0	0.9239	0.7071	0.3827	0.0
$\phi(0.10, \xi)$	0.0	0.1182	0.2861	0.3577	0.3851
$\phi_{16}(0.10, \xi)$	0.0	0.08447	0.2504	0.3584	0.3885
% Error	0.0	28.5	12.5	0.20	0.88
$\phi_{24}(0.10, \xi)$	0.0	0.08443	0.2503	0.3582	0.3886
% Error	0.0	28.6	12.5	0.14	0.91
Finite Difference (0.01 radial spacing)	0.0	0.1115	0.2990	0.3864	0.3991
% Error	0.0	5.7	4.5	8.0	3.6

Transient Temperature Profile of a Wire Filament

Electrically Heated

The problem considered is the transient temperature profile of a cylindrical wire filament electrically heated with only radiative heat losses considered. It is assumed that the physical properties of the wire are constant. The governing equation is

$$\frac{\partial T}{\partial t} = \alpha \frac{\partial^2 T}{\partial x^2} + \beta (T_m^4 - T^4) \quad (39)$$

where

$$\alpha = \frac{k}{c\delta} ; \text{ thermal diffusivity}$$

and

$$\beta = \frac{p\epsilon\sigma}{c\delta\omega}$$

$$T_m = \left(\frac{I^2 \rho}{\omega p \epsilon \sigma} + T_0^4 \right)^{1/4}$$

k is the thermal conductivity, c is the specific heat capacity of the filament material, δ is the density, p is the periphery of the cross section of the filament, ϵ is the total emissivity of the surface, σ is the Stefan-Boltzmann constant, ω is the cross section area, I is the heating current, ρ is the specific resistance and T_0 is the temperature of the chamber walls in which the heating is occurring. The following I.C. and B.C.'s were assumed:

I.C.

$$T(x,0) = T_0 ; \quad -1 < x < 1 \quad (40)$$

B.C.'s

$$T(1,t) = T(-1,t) = T_0 ; \quad t > 0 \quad (41)$$

An analytic solution for the central region of the wire is given by Jain and Krishnan [1955]

$$\frac{T_m - T}{T_m + T} \exp[-2 \tan^{-1} \left(\frac{T}{T_m} \right)] = C \exp \left[- \frac{t}{t_0} \right] \quad (42)$$

where

$$t_0 = (4\beta T_m^3)^{-1}$$

and

$$C = \frac{T_m - T_0}{T_m + T_0} \exp[-2 \tan^{-1} \left(\frac{T_0}{T_m} \right)]$$

The system was modeled for a wire two centimeters(cm) in length with $\alpha = 0.1$, $\beta = 8.6 \times 10^{-11}$, $T_m = 1182.5^\circ\text{K}$, $T_0 = 281^\circ\text{K}$, $t_0 = 1.762$ and $C=0.3863$. The temperature profile obtained for a time of 0.04 seconds is displayed in Figure 1. This profile was obtained for both pseudospectral and finite difference representations using a second order Adams-Bashforth predictor with time increments of 0.0001 seconds. The values obtained from the numerical solutions for the central region of the wire agree exactly with that obtained from the analytic solution. The finite difference representation, with nodes spaced 0.01 cm and using symmetry about $x=0$, required approximately 1.17 seconds per iteration on a Zenith Z-122 microcomputer using compiled Basic. Approximately 0.42 seconds per iteration was required for a twenty-five term pseudospectral representation on the same machine. In both cases

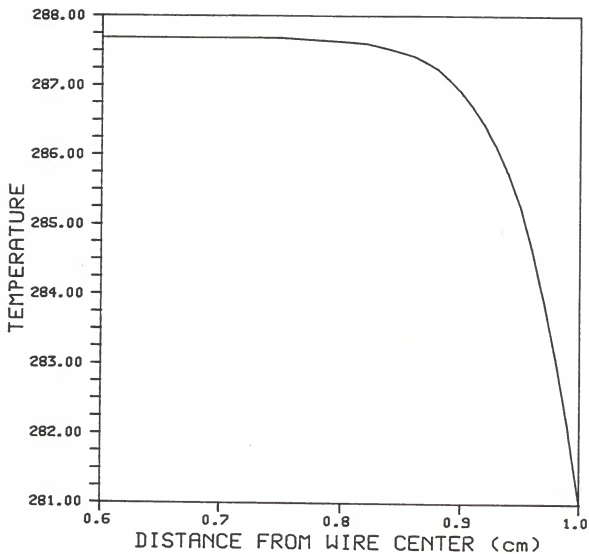


Figure 1. Temperature Profile within an Electrically Heated Wire Filament Obtained with Finite Difference and Pseudospectral Methods for $t=0.04$ seconds.

the number of terms retained for the physical representation may be reduced without affecting the accuracy of the numerical solution, thus increasing the speed of the computation.

The Classical Graetz Problem

The classical Graetz problem refers to the analysis of laminar flow heat transfer in a tube. For the case of a circular tube the following conditions are assumed; 1) The heat capacity, thermal conductivity, viscosity, and density of the fluid are constant; 2) The laminar velocity profile is established before entering the region in which heat transfer will occur; 3) At $x=0$ the wall temperature will change from that of the uniform fluid temperature, T_0 , to the new value, T_w , and is constant at this value for $x>0$. The governing equation for the heat transfer occurring in a cylindrical tube neglecting thermal conduction along the axis is

$$u \frac{\partial T}{\partial x} = \frac{k}{C_p \rho} \left[\frac{1}{r} \frac{\partial}{\partial r} \left(r \frac{\partial T}{\partial r} \right) \right] \quad (43)$$

where u is the velocity at the radial position r , k is the thermal conductivity, C_p is the heat capacity, ρ is the density of the fluid, T is the local temperature and x is the axial position. The laminar velocity profile is defined to be

$$u = 2U \left[1 - \left(\frac{r}{r_w} \right)^2 \right] \quad (44)$$

U is the maximum velocity, r_w is the radial distance to the wall. Boundary conditions employed are

$$T(r,0) = T_0; \quad 0 < r < r_w \quad (45)$$

$$T(r_w, x) = T_w; \quad x > 0 \quad (46)$$

$$\frac{\partial T(0, x)}{\partial r} = 0 \quad x > 0 \quad (47)$$

The solution takes the form:

$$\frac{T_w - T}{T_w - T_0} = \sum_{n=0}^{\infty} c_n \phi_n \left(\frac{r}{r_w}\right) \exp\left[-\frac{\beta_n^2 \left(\frac{x}{r_w}\right)}{Pe}\right] \quad (48)$$

the values for c_n , ϕ_n and β_n are given by Knudsen and Katz [1958] for $n=0,1$ and 2 which is sufficient for most situations. The governing equation was integrated using a second order Adams-Bashforth method with axial increments of 1×10^{-5} . It was found by trial and error that within the first 30 steps larger axial increments (e.g. doubling the increment size) resulted in numerical instability. A digital filter of the form

$$f'(x) = (f(x+2h) + 2f(x+h) + 9f(x) + 2f(x-h) + f(x-2h))/15 \quad (49)$$

was used initially to damp oscillations occurring from the presence of a discontinuity at the entrance. This filter was modified to account for the variable node spacing that results for Chebyshev representations

$$f'(x_i) = (\delta_2 f(x_{i-2}) + \delta_1 f(x_{i-1}) + 9f(x_i) + 2f(x_{i+1}) + f(x_{i+2})) / (12 + \delta_1 + \delta_2) \quad (50)$$

where

$$\delta_1 = 2(x_i - x_{i-1}) / (x_{i+1} - x_i)$$

and

$$\delta_2 = (x_{i-2} - x_i) / (x_i - x_{i+2})$$

for $i > 1$. For $i=1$ the following filter was used

$$f'(x_1) = (0.25 f(x_0) + 10 f(x_1) + f(x_2)) / 11.25 \quad (51)$$

Weighting was chosen such that the boundary condition at the wall was not over emphasized by the filter. The filters were used only for the first seven axial increments. Figure 2 presents numerical results in relation to values obtained from the series summation with $x/r_w = 0.075$.

It can be seen that good agreement is obtained considering the existence of a discontinuity at the entrance region. More accurate results may possibly be obtained by the use of different filtering methods, different axial spacing between filterings or the use of more accurate integration methods once away from the entrance region. Ku and Hatziaivramidis [1984] examined the classical Graetz problem using Chebyshev pseudospectral representation in the radial direction and either a Chebyshev finite difference or Chebyshev finite element method in the axial direction. The use of Chebyshev techniques in the axial direction was accomplished by transforming the problem from an infinite domain on the x -axis to a finite domain. The transformation

$$z = \frac{1}{\pi} \tan^{-1} \left(\frac{x}{\kappa r_w} \right) \quad (52)$$

mapped the problem onto a domain of $z = \pm 0.5$, where κ is a constant that may be varied at will. Both the Chebyshev finite difference and finite element techniques gave excellent results in general.

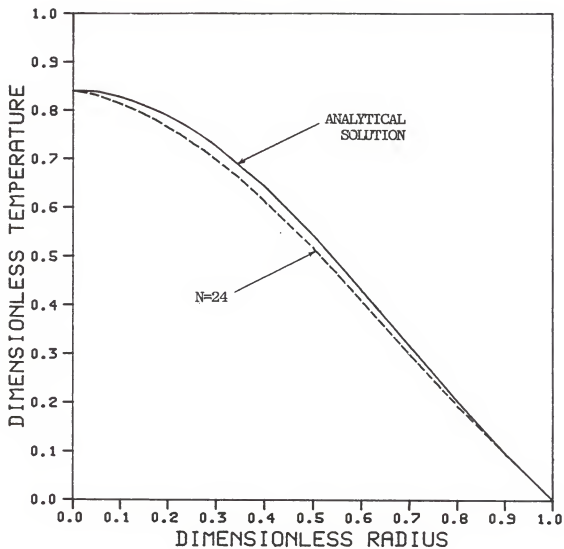


Figure 2. Solutions to the Classical Graetz Problem from the Analytic Series Summation and the Pseudospectral Method for $x/r_w = 0.075$.

Diffusion in a Planar Slab

This problem considers the transient diffusion of ethanol in a porous planar slab with concentration-dependent diffusivity. Values for the diffusivity of ethanol in water (Bird et. al. [1960]) were fit to a third order power series of the form

$$D = a + bX_E + cX_E^2 + dX_E^3 \quad (53)$$

where $a = 1.443935 \times 10^{-5}$

$$b = -7.373196 \times 10^{-5}$$

$$c = 1.615881 \times 10^{-4}$$

$$d = -7.973184 \times 10^{-5}$$

as determined with a statistical software package (3-D Designer Statistics for Micros) where D is diffusivity and X_E mole fraction of ethanol. The governing equation for transient diffusion of ethanol in a slab infinite along the x and z axes is

$$\frac{\partial X_E}{\partial t} = \frac{dD}{dy} \frac{\partial X_E}{\partial y} + D \frac{\partial^2 X_E}{\partial y^2} \quad (54)$$

An expression relating the derivative of the diffusivity to ethanol mole fraction can be introduced through the chain rule

$$\frac{dD}{dy} = \frac{dD}{dX_E} \frac{\partial X_E}{\partial y} \quad (55)$$

Therefore the governing equation can be expressed in terms of ethanol

mole fraction only

$$\frac{\partial X_E}{\partial t} = (b + 2cX_E + 3dX_E^2) \left(\frac{\partial X_E}{\partial y}\right)^2 + (a + bX_E + cX_E^2 + dX_E^3) \frac{\partial^2 X_E}{\partial y^2} \quad (56)$$

Initial and boundary conditions impressed upon a slab 2 centimeters thick are

$$X_E(y, 0) = 1; \quad -1 < y < 1 \quad (57)$$

$$X_E(+1, t) = X_E(-1, t) = 0; \quad t > 0 \quad (58)$$

Both a second-order Adams-Bashforth and a fourth-order Runge-Kutta scheme were used to integrate the governing equation. Chebyshev representations of 17, 25 and 33 terms were used to evaluate the solution in addition to a finite difference method used for comparison. A second-order Adams-Bashforth method was initially applied with digital filtering to evaluate the governing equation. This particular technique displayed severe discrepancies from the finite difference solution and even among the various pseudospectral solutions. Integrating to $t=1000$ seconds invariably led to the first term, away from the wall, being approximately 0.62 ± 0.02 for each approximation. Subsequently, a fourth-order Runge-Kutta method was applied to assess the validity of the Adams-Bashforth method that was used. This approach gave the same results as the Adams-Bashforth method to within 5%. Integrating to $t=5000$ seconds, with 17 terms, still resulted in the term next to the wall being approximately 0.62 ± 0.02 . This would suggest the pseudospectral approximation in the vicinity of the wall was near its steady state value for the above approach.

Examination of the governing equation suggests that the first and second derivatives and the evaluation of the diffusivity terms control the solution. Therefore, the validity of the approximations for derivatives was examined. Due to the presence of initial discontinuities at both boundaries, the derivative approximations oscillated about the correct derivative values. Oscillations were most severe at the boundaries and attenuated as the central region was approached. Since the derivative values initially should have been zero in the core region both positive and negative deviations about the correct solution were introduced; thus the digital filter that was used for the Graetz problem was applied to both the first and second derivatives. This approach produced reasonable results in comparison to the finite difference values.

Figures 3 and 4 in addition to Tables 3 and 4 display the results obtained. These results are for a second-order Adams-Bashforth predictor with step sizes of 1, 2.5 and 10 seconds for 33, 25 and 17 term representations respectively. The derivatives were filtered for the first 500 seconds, in addition a "cut-off" filter was used. Typically, due to the oscillation of the derivative values, the solution also oscillated to a lesser degree, most noticeably when the true solution was constant. Therefore when the collocation approximation for mole fraction exceeded one, that point along with the succeeding points were set equal to one, thus "cutting-off" oscillatory behavior. The finite difference representation used nodes spaced 0.005 cm apart and symmetry about $x=0$ with the integration being carried out by a second-order Adams-Bashforth method with time increments of 0.5 seconds.

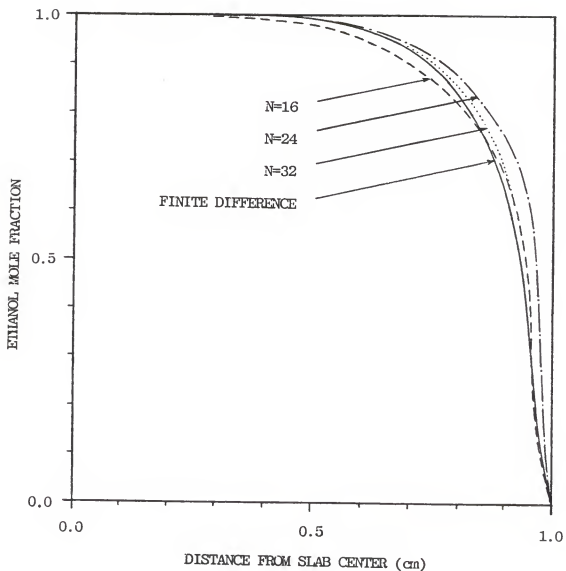


Figure 3. Ethanol concentration Profiles within a Slab Obtained by a Finite Difference Representation and Pseudospectral Representations of 17, 25, and 33 Terms, for $t=1000$ seconds.

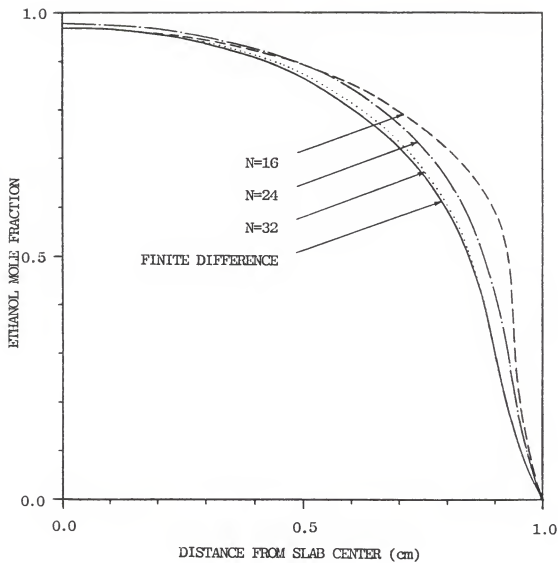


Figure 4. Ethanol concentration Profiles within a Slab Obtained by a Finite Difference Representation and Pseudospectral Representations of 17, 25, and 33 Terms, for $t=5000$ seconds.

Table 3. Comparison of ethanol mole fractions at various points within a slab at a time of 1000 seconds for finite difference (FD) and pseudospectral methods.

	x(cm)			
	0.9239	0.7071	0.3827	0
ϕ_{FD}	0.5357	0.9281	0.9984	1
ϕ_{16}	0.5982	0.8958	0.9910	1
% Error	11.67	3.480	0.7412	0
ϕ_{24}	0.7094	0.9355	0.9991	1
% Error	32.42	0.7973	0.07011	0
ϕ_{32}	0.6157	0.9295	0.9979	1
% Error	14.93	0.1509	0.05008	0

Table 4. Comparison of ethanol mole fractions at various points within a slab at a time of 5000 seconds for finite difference (FD) and pseudospectral methods.

	x(cm)			
	0.9239	0.7071	0.3827	0
ϕ_{FD}	0.1954	0.7188	0.9116	0.9695
ϕ_{16}	0.5066	0.7844	0.9210	0.9665
% Error	159.3	9.126	1.031	0.3094
ϕ_{24}	0.3316	0.7627	0.9295	0.9770
% Error	69.70	6.107	1.964	0.7736
ϕ_{32}	0.1980	0.7233	0.9151	0.9708
% Error	1.331	0.6260	0.3839	0.1341

Figure 3 displays the pseudospectral and finite difference approximations for $t=1000$ seconds. Table 3 compares error between finite difference and pseudospectral methods. It can be seen that the 33 term series representation results in the best approximation to the solution. In addition Table 3 substantiates this view point by comparison of relative percent error. Figure 4 and Table 4 present the results for $t=5000$ seconds. Again it is seen that the 33 term representation accurately approximates the finite difference solution.

It is apparent from the deviations among the approximate solutions that the 17 and 25 term expansions cannot adequately represent the initial solution. Although, no effort was made to optimize the filtering, it is likely that the derivative values require far less filtering than was applied.

Diffusion and Reaction in a Spherical Pellet

The problem considered was the diffusion and concurrent reaction of a substrate within a spherical catalysis pellet with nonlinear Michaelis-Menton kinetics. It is assumed that the pellet is homogeneous with diffusion and reaction symmetric such that only radial variation need be considered. In addition, diffusivity and density of the system are assumed to be constant. The governing equation is:

$$\frac{\partial S}{\partial t} = D \left(\frac{1}{r^2} \frac{\partial}{\partial r} \left(r^2 \frac{\partial S}{\partial r} \right) \right) - \frac{V_m S}{K_m + S} \quad (59)$$

S is substrate concentration, D is the diffusivity of the substrate within the pellet, r is radial position, V_m the maximum rate at which

the reaction can take place with respect to the physical conditions (i.e. temperature) and K_m a kinetic constant. The following dimensionless variables are introduced into the governing equation

$$C = \frac{S}{S_b} ; \quad R = \frac{r}{r_s} ; \quad \tau = \frac{tD}{r_s^2}$$

S_b is the bulk concentration of substrate and r_s is the radial distance to the pellet surface. Which results in

$$\frac{\partial C}{\partial \tau} = \frac{\partial^2 C}{\partial R^2} + \frac{2}{R} \frac{\partial C}{\partial R} - \frac{\alpha C}{\beta + C} \quad (60)$$

where

$$\alpha = \frac{V_m r_s^2}{S_b D} ; \quad \beta = \frac{K_m}{S_b}$$

The initial and boundary conditions considered are:

$$C(r,0) = 0; \quad 0 < r < 1 \quad (61)$$

$$C(1,t) = 1; \quad t > 0 \quad (62)$$

$$\frac{\partial C(0,t)}{\partial r} = 0; \quad t > 0 \quad (63)$$

Due to the nonlinear nature of this problem, no analytic solution is known to exist. Therefore, a finite difference method was executed for comparison. The governing equation was integrated using a second order Adams-Bashforth method. The initial thirty increments were 1×10^{-5} in size at which point the time increment was increased to 1×10^{-4} . The use of small initial time increments was to damp the oscillations present in the solution arising from the initial discontinuity and ease the effects that filtering may have on the ultimate solution. The values

R	$C_{FD}(r, 0.025)$	$C_I(R, 0.025)$	$C_{II}(R, 0.025)$	C_{FD-I}	C_{FD-II}	$C_I - C_{II}$	% Difference $(\frac{ C_1 - C_2 }{C_1} \times 100)$	
							C_{FD-I}	C_{FD-II}
1	1	1	1	0	0	0	0	0
0.9239	0.7710	0.7806	0.7795	1.25	1.10	0.141		
0.7071	0.2436	0.2666	0.2635	9.44	8.17	1.16		
0.3827	0.01277	0.02171	0.01955	70.0	5.31	9.95		
0	3.448×10^{-4}	9.940×10^{-4}	2.005×10^{-4}	188.	41.9	79.8		

Table 5. Concentration profile within a spherical pellet at $r = 0.025$ determined by finite difference (FD) and pseudospectral approximations using filtering schemes I and II.

R	C	C _I	C _{II}
1	1	1	1
0.9808	0.1411	0.2212	0.1740
0.9239	-7.843x10 ⁻³	0.1226	0.09500
0.8315	2.027x10 ⁻³	0.04517	0.02741
0.7071	-8.452x10 ⁻⁴	0.01841	8.861x10 ⁻³
0.5556	4.737x10 ⁻⁴	6.421x10 ⁻³	2.173x10 ⁻³
0.3827	-3.270x10 ⁻⁴	2.105x10 ⁻⁴	4.382x10 ⁻⁴
0.1951	2.657x10 ⁻⁴	7.139x10 ⁻⁴	1.155x10 ⁻⁴
0	-1.563x10 ⁻⁴	3.347x10 ⁻⁴	2.265x10 ⁻⁵

Table 6. A comparison of concentration profiles within a spherical pellet after seven time increments for no filtering and filtering schemes I and II.

chosen for α and β were 7.5 and 1, respectively; these values indicate that for a region in which the substrate concentration is high (i.e. $C \rightarrow 1$), the kinetics are nonlinear and for the case where the concentration is low, first-order kinetics hold. The filters are the same as those used with the Graetz problem with the exception of weighting on the central point, which was increased by one for both filters. Two separate filtering approaches were used, the first (I) filtered the first seven increments, the second (II) filtered at increments seven and fourteen until no negative concentrations existed. It can be seen from Table 5 that significant differences can occur from the use of different filtering schemes, most notably in the central region where the solution approaches zero. The question that arises, however, is the extent to which filtering affects the numeric values. Table 6 presents concentration values with no filtering and filtering schemes I and II at increment seven. It can be seen there are noticeable differences between the results of the two methods. Note the oscillations present without filtering, these oscillations occur due to the presence of the discontinuity at the boundary and increase at each time step leading ultimately to numeric instability.

External Separated Flows

One of the original goals of this research was the application of pseudospectral methods to external separated flows, notably flow about a pitched flat plate. Although this problem is extremely difficult, it is nevertheless instructive. Therefore, consider the two dimensional incompressible Navier-Stokes equation for flow past a pitched flat plate expressed in terms of the stream function

$$\frac{\partial}{\partial t} \nabla^2 \psi + (\psi_y \frac{\partial}{\partial x} - \psi_x \frac{\partial}{\partial y}) \nabla^2 \psi = \nu \nabla^4 \psi \quad (64)$$

The transient response of the flow to a periodic forcing function is the ultimate goal, but the first step is to consider the steady state solution. A Fourier spectral solution for the steady state form of equation (64) was presented by Mei and Plotkin [1984] for confined laminar wakes. The use of the Fourier spectral method by Mei and Plotkin was made possible by imposition of periodic boundary conditions.

As a preliminary step, the Falkner-Skan equation was used to estimate the accuracy of the pseudospectral approximation for separated flow present on a divergent wall. Based upon a fourth order Runge-Kutta solution of the Falkner-Skan equation ($\beta = -0.125$)

$$f''' + ff'' + \beta(1-f')^2 = 0 \quad (65)$$

with boundary conditions

$$f = f' = 0; \quad \eta = 0$$

$$f' = 1; \quad \eta = \infty \quad (66)$$

a Chebyshev interpolation function was evaluated for 11, 21, and 41 term representations. The evaluation was based on a comparison of the first and second derivatives found using a pseudospectral evaluation and those obtained by the Runge-Kutta method. The coefficients for the pseudospectral approximation are obtained by Fourier transformation. Three separate observations were made from these evaluations; 1) In one trial the data used for the value of $f(\eta)$ at each collocation point was rounded to three significant figures with $N=20$. This resulted in large oscillations of the first derivative, as noted by Osher [1984] and Majda et al. [1978]. 2) Increasing the number of collocation points from 11 to

21 to 41 did not significantly affect the accuracy of the resulting approximations. 3) The accuracy of a derivative decreased approximately one order of magnitude for each increase in the order of differentiation. It should be noted however, that the decrease in accuracy of succeeding derivatives may be due to slight errors introduced by the use of linear interpolation to evaluate point values for the pseudospectral approximation. A compilation of these results is presented in Tables 7 and 8.

Based upon the above, it was decided to use a steady state stream function-vorticity representation for the flow.

$$\frac{\partial \omega}{\partial x} \frac{\partial \psi}{\partial y} - \frac{\partial \omega}{\partial y} \frac{\partial \psi}{\partial x} = \nu \left(\frac{\partial^2 \omega}{\partial x^2} + \frac{\partial^2 \omega}{\partial y^2} \right) \quad (67)$$

$$\omega = -\frac{1}{2} \left(\frac{\partial^2 \psi}{\partial x^2} + \frac{\partial^2 \psi}{\partial y^2} \right) \quad (68)$$

with the boundary conditions

$$\psi(x, 0) = \psi_x(x, 0) = \psi_y(x, 0) = 0 \quad -a < x < a \quad (69)$$

$$\psi(x, \pm\infty) = \psi(\pm\infty, y) = \psi_{\text{free stream}} \quad (70)$$

$$\omega(\pm\infty, y) = \omega(x, \pm\infty) = 0 \quad (71)$$

$$\omega(x, 0) = -\frac{1}{2} \frac{\partial^2 \psi}{\partial y^2} \quad -a < x < a \quad (72)$$

Then the stream function and vorticity can be approximated by:

$\eta f'(\eta)$	RK	N=10	N=20	N=20 (3 significant figures)	N=40
0.1958	-0.025576	-0.024552	-0.024773	-0.023739	-0.023847
0.7639	-0.072826	-0.074226	-0.072494	-0.084111	-0.073005
1.649	-0.067062	-0.0654990	-0.066957	-0.079243	-0.067009
2.764	0.0886210	0.086654	0.088983	0.071295	0.088778
4.000	0.45786	0.45962	0.45794	0.45309	0.45790
5.236	0.84314	0.84205	0.84291	0.85391	0.84302
6.351	0.98166	0.98236	0.98171	0.94579	0.98163
7.236	0.99963	0.99931	0.99964	1.05521	0.99965
7.804	1.00106	1.00118	1.00105	1.07258	1.00111
8.000	1.00116	1.00101	1.00119	0.95798	1.00130

Table 7 : Comparisons of the first derivative of the Falkner-Skan equation for a 4th order Runge-Kutta method and Chebyshev collocation where N represents the number of terms retained in the series expansion.

$\eta''(\eta)$	RK	N=10	N=20	N=20 (3 significant figures)	N=40
0.1958	-0.11855	-0.11514	-0.13321	0.14046	-0.13404
0.7639	-0.04837	-0.04922	-0.04922	-0.02698	-0.04577
1.649	0.06256	0.06346	0.06193	0.07137	0.05968
2.764	0.22016	0.21912	0.21990	0.18439	0.22008
4.000	0.35247	0.35299	0.35490	0.21807	0.35865
5.236	0.22321	0.22364	0.22300	0.17815	0.22307
6.351	0.04637	0.04527	0.04592	-0.09232	0.04413
7.236	0.00537	0.06317	0.00530	-0.14462	0.00500
7.804	8×10^{-4}	-1.1×10^{-4}	7.5×10^{-4}	0.68487	6.5×10^{-4}
8.000	3.5×10^{-4}	-0.00103	0.00121	-2.82886	0.00721

Table 8: Comparisons of the second derivative of the Falkner-Skan Equation for a 4th order Runge-Kutta and Chebyshev collocation where N represents the number of terms retained in the series expansion.

$$\psi(x, y_j) = \sum_{n=0}^N a_n(x) T_n(y_j) \quad (73)$$

$$\omega(x, y_1) = \sum_{n=0}^N \alpha_n(x) T_n(y_1) \quad (74)$$

This representation was chosen to make use of the increased accuracy of pseudospectral approximations along the axis in which the greatest amount of change will occur; Gottlieb et al. [1984a] note that a finite difference representation is typically used along the vertical axis and a pseudospectral representation along the horizontal axis. The solution is split into an upper and lower region for above and below the plate and having the numerical boundary conditions

$$\omega^u(x, 0) = \omega^l(x, 0) \quad a < x < -a \quad (75)$$

$$\psi^u(x, 0) = \psi^l(x, 0) \quad a < x < -a \quad (76)$$

where the superscript u and l refer to the upper and lower regions respectively.

The following computational scheme was then used to evaluate the flow. The mesh nodes for the stream function were initialized using an equation given by Lamb [1945] that had been corrected for the angle of attack and transformed to Cartesian coordinates (Appendix A). The vorticity was initialized at zero everywhere except on the plate where a first order finite difference evaluation was performed based on methods found in Roache [1972]

$$\omega(x, 0) = \frac{2(\psi_{w+1} - \psi_w)}{\Delta n} + 0(\Delta n) \quad (77)$$

where Δn is the distance from the wall (w) to the mesh node normal to the wall ($w+1$). The following steps were then followed in obtaining a solution:

1) Determine the pseudospectral coefficients to the Chebyshev polynomials at each (x, y_j) combination.

2) Starting at the leading edge of the flow field evaluate the derivatives with respect to y for that column.

3) Equation (67) is solved with respect to ω for a finite difference representation of the x derivative.

4) Equation (68) is solved with respect to ψ for a finite difference representation of the x derivative.

5) Steps 3) and 4) are repeated for each value of ω and ψ in the column.

6) Move to the next column and repeat steps 2) through 5).

7) Repeat for the second region.

8) Satisfy the numerical boundary conditions.

9) Continue steps 1) through 8) until convergence is achieved.

In order to estimate the accuracy of the above algorithm a central finite difference algorithm for the stream function representation was developed. The successive under relaxation algorithm was based on the same boundary conditions as given by equations (69)-(70).

Both the finite difference and pseudospectral algorithms were explosively unstable. The fact that both algorithms were unstable suggests that improper boundary conditions are being applied. Either boundary condition for the derivative of the stream function on the

plate may cause problems. These boundary conditions have to be satisfied since each represents a velocity component on the plate and the Newtonian no-slip condition requires that velocity be zero at the surface. Evaluating either condition with a forward finite difference approximation implies that the entire region around the plate has $\psi = 0$. As an aside, insufficient numerical boundary conditions were applied for the pseudospectral approximation. The first and second derivatives for both stream function and vorticity should have been equated across the boundary.

Chapter IV. CONCLUSIONS

The objective of this work was to assess the suitability and computational efficiency of the application of spectral methods to problems in transport phenomena. This was accomplished by the evaluation of representative problems from each major area of transport phenomena; momentum, mass and heat transfer.

It was found that Chebyshev pseudospectral representations can accurately evaluate derivatives of smooth functions with few expansion terms. The reduction in the number of nodes at which a solution was sought, along with the use of matrices to evaluate derivatives resulted in significantly faster solution times than obtained with finite difference representations of corresponding accuracy. The presence of a discontinuity in the solution domain was found to be a serious problem for a number of initial and boundary value problems. A discontinuity affects the entire solution domain due to the global nature of derivative evaluation. The effects of this problem can be removed by the use of digital filtering; such filters were found to be quite satisfactory in the removal of "noise" from the solution arising from a discontinuity. Therefore, pseudospectral methods should be applicable to many if not most problems of interest in transport phenomena.

There is need to develop criteria for the application of filters to pseudospectral solutions, namely the type of filter that should be applied and amount of filtering necessary to arrive at accurate results for a given type of problem. Additionally, filters that retain the "infinite" order accuracy of spectral methods are desirable. Finally, for problems in which a discontinuity is present due to initial

conditions, other methods for initializing the solution should be investigated so that the discontinuity can be removed and the accuracy of the pseudospectral method exploited. An example of alternative initialization would be the use of a high order finite difference method to remove the discontinuity and subsequent use of an accurate interpolation technique to provide solution values for the pseudospectral points.

APPENDIX A

STREAMLINE EXPRESSION FOR A PITCHED FLAT PLATE

Lamb [1945] gives the following representation for the stream function for flow past a flat plate pitched at angle of 45°

$$\psi = -\frac{cq_0}{\sqrt{2}} \sinh\xi(\cos\eta - \sin\eta) \quad (A1)$$

whose edges are located at $x = \pm c$ and where q_0 is the free stream velocity. This equation was derived from the relation describing fluid motion relative to an elliptic cylinder

$$\psi = -c \left\{ v \sinh\xi \cos\eta - u \sinh\xi \sin\eta \right\} \quad (A2)$$

where u and v are the x and y components of velocity with respect to the plate. Then ψ can be represented as

$$\psi = -c q_0 \cos\theta \sinh\xi \left\{ \tan\theta \cos\eta - \sin\eta \right\} \quad (A3)$$

where θ is the angle of attack for the plate. Cartesian coordinates and elliptic coordinates are related in the following fashion

$$x = c \cosh(\xi) \cos(\eta) \quad (A4)$$

$$y = c \sinh(\xi) \sin(\eta) \quad (A5)$$

The following relation

$$\frac{x^2}{c^2 \cos^2 \eta} - \frac{y^2}{c^2 \sin^2 \eta} = 1 \quad (A6)$$

along with the definition of a point on a hyperbola and the relation of \sinh to \cosh define the following relations for the stream function in Cartesian coordinates

$$\psi = -q_0 \cos\theta \left\{ \tan\theta \sqrt{x^2 - \frac{1}{4}(\sqrt{(c+x)^2 + y^2} - \sqrt{(c-x)^2 + y^2})^2} - y \right\} \quad (A7)$$

for $y > 0$, and

$$\psi = q_0 \cos\theta \left\{ \tan\theta \sqrt{x^2 - \frac{1}{4}(\sqrt{(c+x)^2 + y^2} - \sqrt{(c-x)^2 + y^2})^2} - y \right\} \quad (A8)$$

for $y < 0$.

APPENDIX B
COMPUTER PROGRAMS

The programs in this Appendix represent each section of Chapter III. Two programs have been used for the evaluation of the derivative matrix defined by equation (32) given N , where there are $N+1$ terms in the series expansion (0 to N). All programs, with the exception of one, have been written in Basic due to the availability of interpretive and compiler versions of this language for microcomputers. The one exception was written in Fortran. The programs should be self explanatory with the remarks provided in each.

```

C THE FOLLOWING PROGRAM EVALUATES MATRICES FOR THE
C DETERMINATION OF DERIVATIVE COEFFICIENTS.
  REAL A(33,33),B(33,33),C(33,33),D(33,33)
  DATA A,B,C,D/1089*0.,1089*0.,1089*0.,1089*0./
  DATA L,M,N,IA,IB,IC/33,33,33,33,33,33/
  OPEN(1,FILE='C1.DAT')
  OPEN(2,FILE='C2.DAT')
C   OPEN(3,FILE='C3.DAT')
C   OPEN(4,FILE='C4.DAT')
  WRITE(*,753)
753  FORMAT(' N?')
  READ(*,754)N
754  FORMAT(I2)
  INDEX=2
  AINDEX=N-2
  BINDEX=N-2
  DO 10 I=1,N
    TI=I
    DO 20 J=INDEX,N,2
      A(I,J)= 2.*(N-1.-BINDEX)
      BINDEX=BINDEX - 2.
      IF (J.EQ.N-1) GOTO 16
      GOTO 20
16   IF (2*(I/2).NE.I) GOTO 15
20  CONTINUE
15  INDEX=INDEX+1
    IF (INDEX.GT.N) GOTO 26
    BINDEX=AINDEX-TI
10  CONTINUE
26  CALL VMULFF(A,A,L,M,N,IA,IB,B,IC,IER)
    CALL VMULFF(A,B,L,M,N,IA,IB,C,IC,IER)
    CALL VMULFF(B,B,L,M,N,IA,IB,D,IC,IER)
  DO 30 I=1,N
    A(1,I)=A(1,I)/2.
    B(1,I)=B(1,I)/2.
    C(1,I)=C(1,I)/2.
30  D(1,I)=D(1,I)/2.
  DO 90 I=1,N
    DO 90 J=1,N
      WRITE(1,1000)A(I,J)
      WRITE(2,1000)B(I,J)
C     WRITE(3,1000)C(I,J)
C     WRITE(4,1000)D(I,J)
  90  CONTINUE
1000 FORMAT(F15.2)
  STOP
  END

```

```

1 / THE FOLLOWING PROGRAM DETERMINES THE MATRIX FOR THE
2 / DIRECT EVALUATION OF DERIVATIVES FROM SOLUTION VALUES
10 CLS
15 PI#=3.141592654#
16 N=32
20 DIM C1(33,33),C2(33,33),T1(33,33),T2(33,33)
21 DIM TT(33,33),TC(33,33)
30 OPEN "I",1,"C1.DAT"
40 OPEN "I",2,"C2.DAT"
50 FOR I=0 TO N
60     FOR J=0 TO N
70         INPUT#1,C1(I,J)
80         INPUT#2,C2(I,J)
90     NEXT J
100 NEXT I
110 FOR I=0 TO N
120     IF I=0 OR I=N THEN C1=2 ELSE C1=1
130     FOR J=0 TO N
140         IF J=0 OR J=N THEN C2=2 ELSE C2=1
150         TT(I,J)= 2*COS(I*J*PI#/N)/N/C1/C2
160         TC(J,I)=COS(I*J*PI#/N)
170     NEXT J
180 NEXT I
190 FOR I=0 TO N
200     FOR J=0 TO N
210         T1(I,J)=0:T2(I,J)=0
220         FOR K=0 TO N
230             T1(I,J)=T1(I,J) + C1(I,K)*TT(K,J)
240             T2(I,J)=T2(I,J) + C2(I,K)*TT(K,J)
250         NEXT K
260     NEXT J
270 NEXT I
280 FOR I=0 TO N
290     FOR J=0 TO N
300         C1(I,J)=0:C2(I,J)=0
310         FOR K=0 TO N
320             C1(I,J)=C1(I,J) + TC(I,K)*T1(K,J)
330             C2(I,J)=C2(I,J) + TC(I,K)*T2(K,J)
340         NEXT K
350     NEXT J
360 NEXT I
370 OPEN "O",3,"G1N32.DAT"
380 OPEN "O",4,"G2N32.DAT"
390 FOR I=0 TO N
400     FOR J=0 TO N
410         PRINT#3,C1(I,J)
420     NEXT J
430 NEXT I
440 FOR I=0 TO N
450     FOR J=0 TO N
460         PRINT#4,C2(I,J)
470     NEXT J
480 NEXT I

```

490 CLOSE

```
1 ' The following program calculates the start-up velocity
2 ' profile in a circular tube using Chebyshev pseudo-
3 ' spectral method.
10 CLS
20 DIM V(25),G1(25,25),G2(25,25),VP(25),VPP(25),FOLD(25)
30 N=24:PI=3.1415926#
40 OPEN "I",1,"G1N24.DAT"
50 OPEN "I",2,"G2N24.DAT"
60 FOR I=0 TO N
70     FOR J=0 TO N
80         INPUT#1,G1(I,J)
90         INPUT#2,G2(I,J)
100     NEXT J
110 NEXT I
120 FOR JFK=1 TO 800
130     GOSUB 300
140     FOR I=1 TO N/2
150         R=COS(I*PI/N):IF R<.00001 THEN R=.00001
160         V(I)=V(I) + .000125*(4 + VP(I)/R + VPP(I))
170     NEXT I
180     FOR I=N/2 TO N
190         V(I)= V(N-I)
200     NEXT I
210     FOR I=0 TO N/2
220         PRINT V(I)
230     NEXT I
240 NEXT JFK
250 LPRINT "N=24 UNSTEADY LAMINAR FLOW IN A CIRCULAR TUBE"
260 FOR I=0 TO N/2
270     LPRINT I,COS(I*PI/N),V(I)
280 NEXT I
290 STOP
300 FOR I=1 TO N/2
310     VP(I)=0:VPP(I)=0
320     FOR J=1 TO N
330         VP(I)=VP(I) + G1(I,J)*V(J)
340         VPP(I)=VPP(I) + G2(I,J)*V(J)
350     NEXT J
360 NEXT I
370 RETURN
```

```

1 * The following program evaluates the transient
2 * temperature profile of a wire electrically heated.
3 * The Chebyshev pseudospectral method is used in this
4 * program.
10 CLS
20 DEFINT I
30 DEFINT J
40 N=24
50 DIM T(60), TFP(60), A(60), APP(60), OLD(60)
60 DIM G2(25, 25)
70 OPEN "I", 1, "G2N24.DAT"
80 FOR I=0 TO N
90   FOR J=0 TO N
100     INPUT #1, G2(I, J)
110   NEXT J
120 NEXT I
130 H=.0001
140 PI=3.1415926#
150 ALPHA=.1
160 BETA=8.5817E-11
170 TM=1.95555E+12
180 T0=281
190 FOR I=0 TO N
200   T(I)=T0
210   OLD(I)=167.28
220 NEXT I
230 LPRINT TIME$
240 FOR JFK=1 TO 400
250   GOSUB 410
260     FOR I=1 TO N/2
270       TEMP= ALPHA*TFP(I) + BETA*(TM - T(I)^4)
280       T(I)= T(I) + H*(3*TEMP - OLD(I))/2
290       OLD(I)=TEMP
300     NEXT I
310     FOR I=1 TO N/2
320       T(N-I)=T(I)
330     NEXT I
340   NEXT JFK
350 LPRINT TIME$
360 OPEN "O", 2, "WIRES.DAT"
370 FOR I=0 TO N/2
380   PRINT #2, COS(I*PI/N), T(I), A$, COS((I+N/2+1)*PI/N),
     T(I+N/2+1)
390 NEXT I
400 STOP
410 FOR I=1 TO N/2
420   TFP(I)=0
430   FOR J=0 TO N
440     TFP(I)=TFP(I) + T(J)*G2(I, J)
450   NEXT J
460 NEXT I
470 RETURN

```

```

1  The following program evaluates the classical Graetz
2  problem for Pe=1 and Re=1.
10 DEFDEL C
20 CLS
30 DIM C(25),CP(25),CPP(25),COLD(25),G1(25,25)
40 DIM C1OLD(25),G2(25,25),CN(25)
50 PI=3.141592654#
60 OPEN"O",3,"GRAETZ.DAT"
70 N=16
80 ALPHA=7.5
90 BETA=1
100 PE=1
110 H=.00001
120 FOR I=1 TO N-1:C(I)=1:NEXT I
130 OPEN"I",1,"G1N16.DAT"
140 OPEN"I",2,"G2N16.DAT"
150 FOR I=0 TO N
160     FOR J=0 TO N
170         INPUT#1,G1(I,J)
180     NEXT J
190 NEXT I
200 FOR I=0 TO N
210     FOR J=0 TO N
220         INPUT#2,G2(I,J)
230     NEXT J
240 NEXT I
250 '*****
260 C(0)=0:C(N)=0
270 FOR JFK=1 TO 7501
280     GOSUB 650
290     FOR I=1 TO N/2
300         R=COS(I*PI/N)
310         IF I=N/2 THEN R=.00005
320         TEMP=(CPP(I)+CP(I)/R)/(1-R^2)/PE
330         C(I)=C(I)+H*(3*TEMP-COLD(I))/2
340         COLD(I)=TEMP
350     NEXT I
360     FOR I=0 TO N/2:'PRINT COS(I*PI/N),C(I)
370     C(N-I)=C(I)
380     CN(I)=C(I)
390     NEXT I
400 'IF JFK=20 THEN GOSUB 670
410 'IF JFK=30 THEN GOSUB 710
420 IF JFK=2500 OR JFK=5000 OR JFK=7500 THEN GOSUB 610
430 IF JFK>7 THEN GOTO 580
440 CN(N/2+1)=C(N/2-1)
450 CN(N/2+2)=C(N/2-2)
460 C(1)=(11*CN(1)+CN(2))/12.25
470 FOR I=2 TO N/2
480     R=COS(I*PI/N)
490     RP1=COS((I+1)*PI/N)
500     RP2=COS((I+2)*PI/N)
510     RM1=COS((I-1)*PI/N)

```

```

520      RM2=COS((I-2)*PI/N)
530      X1= 2*(R - RM1)/(RP1 - R)

540      X2=(RM2 - R)/(R - RP2)
550      C(I)=(X2*CN(I-2)+X1*CN(I-1)+10*CN(I)+2*CN(I+1)
           + CN(I+2))/(13 + X1 + X2)

560      NEXT I
570      FOR I=0 TO N/2:PRINT COS(I*PI/N),C(I),CN(I)
571      C(N-I)=C(I)
575      NEXT I
580 NEXT JFK
590 CLOSE
600 STOP
610 PRINT#3,JFK
620 FOR I=0 TO N/2:PRINT#3,COS(I*PI/N),C(I):NEXT I
630 PRINT#3," "
640 RETURN
650 FOR I=1 TO N/2
660     CP(I)=0
670     CPP(I)=0
680     FOR J=0 TO N
690         CP(I)=CP(I) + G1(I,J)*C(J)
700         CPP(I)=CPP(I) + G2(I,J)*C(J)
710     NEXT J
720 NEXT I
730 RETURN
740 FOR I=0 TO N
750     C1OLD(I)=COLD(I)
760 NEXT I
770 RETURN
780 FOR I=0 TO N
790     COLD(I)=C1OLD(I)
800 NEXT I
810 H=.00005
820 RETURN

```



```

1  ' THE FOLLOWING PROGRAM EVALUATES THE DIFFUSIVITY IN A
2  ' POROUS PLANAR SLAB. THE FIRST AND SECOND DERIVATIVE
3  ' ARE FILTERED WITH A DIGITAL FILTER.
10 DEFINT I
20 DEFINT J
30 CLS
40 DIM C(33), CP(33), CPP(33), COLD(33), G1(33,33)
50 DIM C1OLD(33), G2(33,33), CN(33)
60 PI=3.141592654#
70 N=24
80 A=1.443935
90 B=-7.373196
100 CA=16.15881
110 D=-7.973184
120 H=2
130 OPEN"I",1,"G1N24.DAT
140 OPEN"I",2,"G2N24.DAT
150 FOR I=0 TO N
160     FOR J=0 TO N
170         INPUT#1,G1(I,J)
180     NEXT J
190 NEXT I
200 FOR I=0 TO N
210     FOR J=0 TO N
220         INPUT#2,G2(I,J)
230     NEXT J
240 NEXT I
250 '*****
260 FOR I=1 TO N-1:C(I)=1:NEXT I
270 FOR JFK=1 TO 500
280     GOSUB 670
290     FOR I=1 TO N/2
300         DAB= (A + B*C(I) + CA*C(I)^2 + D*C(I)^3)*.00001
310         DABX= (B + 2*CA*C(I) + 3*D*C(I)^2)*.00001
320         TEMP= DABX*CP(I)^2 + DAB*CPP(I)
330         C(I)= C(I) + H*(3*TEMP - COLD(I))/2
340         COLD(I)=TEMP
350     NEXT I
360     FOR I=0 TO N/2:'PRINT COS(I*PI/N),C(I)
370         IF C(I)>1 THEN CHK=2
380         IF CHK=2 THEN C(I)=1
390         PRINT COS(I*PI/N),C(I)
400         C(N-I)=C(I)
410         CN(I)=C(I)
420     NEXT I
430     CHK=1
440 'IF JFK=98 THEN GOSUB 670
450 'IF JFK=100 THEN GOSUB 710
460 IF 20*CINT(JFK/20)<>JFK THEN GOTO 620
470 IF JFK>0 GOTO 620
480     CN(N/2+1)=C(N/2-1)
490     CN(N/2+2)=C(N/2-2)
500     C(1)= (.25 + 11*CN(1) + CN(2))/12.25

```

```

510     FOR I=2 TO N/2
520         R=COS(I*PI/N)

530         RP1=COS((I+1)*PI/N)
540         RP2=COS((I+2)*PI/N)
550         RM1=COS((I-1)*PI/N)
560         RM2=COS((I-2)*PI/N)
570         X1= 2*(R - RM1)/(RP1 - R)
580         X2= (RM2 - R)/(R - RP2)
590         C(I)= (X2*CN(I-2)+X1*CN(I-1)+10*CN(I)+2*CN(I+1)
                + CN(I+2))/(13 + X1 + X2)

600     NEXT I
610     FOR I=0 TO N/26
611         PRINT COS(I*PI/N), C(I), CN(I)
612         C(N-I)=C(I)
613     NEXT I
620     NEXT JFK
630     OPEN"O", 3, "SLABSH.DAT"
640     FOR I=0 TO N/2:PRINT#3, COS(I*PI/N), C(I):NEXT I
650     CLOSE
660     STOP
670     FOR I=1 TO N/2
680         CP(I)=0
690         CPF(I)=0
700         FOR J=0 TO N
710             CP(I)=CP(I) + G1(I, J)*C(J)
720             CPP(I)=CPP(I) + G2(I, J)*C(J)
730         NEXT J
740         'IF ABS(CPP(I)/CPP(1))<.01 THEN CPP(I)=0
750         'IF ABS(CP(I)/CP(1))<.01 THEN CP(I)=0
760     NEXT I
770     IF JFK>250 THEN RETURN
780     FOR I=0 TO N/2:CN(I)=CP(I):NEXT I
790     CP(1)= (14*CN(1) + CN(2))/15
800     FOR I=2 TO N/2-2
810         R=COS(I*PI/N)
820         RP1=COS((I+1)*PI/N)
830         RP2=COS((I+2)*PI/N)
840         RM1=COS((I-1)*PI/N)
850         RM2=COS((I-2)*PI/N)
860         X1= 2*(R - RM1)/(RP1 - R)
870         X2= (RM2 - R)/(R - RP2)
880         CP(I)= (X2*CN(I-2)+X1*CN(I-1)+13*CN(I)+2*CN(I+1)
                + CN(I+2))/(16+X1+X2)

890     NEXT I
900     FOR I=0 TO N/2:CN(I)=CPP(I):NEXT I
910     CPP(1)= (14*CN(1) + CN(2))/15
920     FOR I=2 TO N/2-2
930         R=COS(I*PI/N)
940         RP1=COS((I+1)*PI/N)
950         RP2=COS((I+2)*PI/N)
960         RM1=COS((I-1)*PI/N)
970         RM2=COS((I-2)*PI/N)

```

```

780      X1= 2*(R - RML)/(RP1 - R)
790      X2= (RM2 - R)/(R - RP2)
1000     CPP(I)=(X2*CN(I-2)+X1*CN(I-1)+13*CN(I)+2*CN(I+1)
          + CN(I+2))/(16+X1+X2)

1010     NEXT I
1020     RETURN

```

```

1 ' The following program evaluates the transient concen-
2 ' tration profile within a spherical nodule in which
3 ' diffusion and reaction is occurring simultaneously.
4 ' The reaction kinetics considered are those proposed
5 ' by Michaelis-Menton for enzymes.
10 CLS
20 DIM C(25),CP(25),CPP(25),COLD(25),G1(25,25)
30 DIM CN(25),G2(25,25),C1OLD(25)
40 PI=3.141592654#
50 N=16
60 ALPHA=7.5
70 BETA=1
80 H=.00001
90 'OPEN"I",1,"G1N16.DAT
100 'OPEN"I",2,"G2N16.DAT
110 FOR I=0 TO N
120     FOR J=0 TO N
130         INPUT#1,G1(I,J)
140     NEXT J
150 NEXT I
160 FOR I=0 TO N
170     FOR J=0 TO N
180         INPUT#2,G2(I,J)
190     NEXT J
200 NEXT I
210 '*****
220 C(0)=1:C(N)=1
230 FOR JFK=1 TO 277
240     GOSUB 580
250     FOR I=1 TO N/2
260         R=COS(I*PI/N)
270         IF I=N/2 THEN R=.00005
280         TEMP=CPP(I)+2*CP(I)/R-ALPHA*C(I)/(BETA+C(I))
290         C(I)= C(I) + H*(3*TEMP - COLD(I))/2
300         'COLD(I)=TEMP
310     NEXT I
320     FOR I=0 TO N/2: PRINT COS(I*PI/N),C(I)
330     C(N-I)=C(I)
340     CN(I)=C(I)
350     NEXT I
360     IF JFK=20 THEN GOSUB 670
370     IF JFK=30 THEN GOSUB 710

```

```

380 IF 7*CINT(JFK/7)=JFK THEN GOTO 381 ELSE GOTO 530
381 IF JFK>14 GOTO 530
385 INDEX=0
390 CN(N/2+1)=C(N/2-1)
400 CN(N/2+2)=C(N/2-2)
410 C(1)= (.25 + 11*CN(1) + CN(2))/12.25
420 FOR I=2 TO N/2
430 R=cos(I*PI/N)
440 RP1=cos((I+1)*PI/N)
450 RP2=cos((I+2)*PI/N)
460 RM1=cos((I-1)*PI/N)
470 RM2=cos((I-2)*PI/N)
480 X1= 2*(R - RM1)/(RP1 - R)
490 X2= (RM2 - R)/(R - RP2)
500 C(I)=(X2*CN(I-2)+X1*CN(I-1)+10*CN(I)+2*CN(I+1)
      +CN(I+2))/(13+X1+X2)
505 IF C(I)<0 THEN INDEX=1
510 NEXT I
515 IF INDEX=1 THEN GOTO 320
520 FOR I=0 TO N/2
521 PRINT cos(I*PI/N),C(I),CN(I)
522 C(N-I)=C(I)
525 NEXT I
530 NEXT JFK
540 OPEN"C",3,"NODP.DAT"
550 FOR I=0 TO N/2:PRINT#3,COS(I*PI/N),C(I):NEXT I
560 CLOSE
570 STOP
580 FOR I=1 TO N/2
590 CP(I)=0
600 CPP(I)=0
610 FOR J=0 TO N
620 CP(I)=CP(I) + G1(I,J)*C(J)
630 CPP(I)=CPP(I) + G2(I,J)*C(J)
640 NEXT J
650 NEXT I
660 RETURN
670 FOR I=0 TO N
680 C1OLD(I)=COLD(I)
690 NEXT I
700 RETURN
710 FOR I=0 TO N
720 COLD(I)=C1OLD(I)
730 NEXT I
740 H=.0001
750 RETURN

```

```

1' THE FOLLOWING PROGRAM ATTEMPTS TO CALCULATE FLOW PAST A
2' PITCHED FLAT PLATE.
10 CLS
20 DIM P(42,26),PX(42,26),FY(42,26),PXX(42,26),PYY(42,26)
30 DIM PXXX(42,26),PYYY(42,26),PXXYY(42,26),PXXY(42,26)
40 DIM PYYT(42),PYYYT(42),FYX(42,26)
50 'OPEN"I",#1,"FPLATE.DAT"
60 INPUT "NUMBER OF ITERATIONS";NUM
70 'FOR I=1 TO 42
80 'FOR J=1 TO 26
90 'INPUT#1,P(I,J)
100 'NEXT J:NEXT I
110 'CLOSE#1
120 NUM=NUM-1
130 CLS
140 MIT=0:H=.6666667:VIS=.17
150 'GOTO 410
160 '***** INITIALIZE NODAL POINT *****
170 FOR I=1 TO 42
180 FOR J=1 TO 26
190 P(I,J)= -1.5625*I + 3.125*J - 3.90625
200 IF J>9 THEN P(I,J)=-1.5625*I +3.125*J + 3.90625
210 NEXT J: NEXT I
220 '***** INITIALIZE POINTS ON THE FLATE *****
230 J= 9
240 FOR I=11 TO 26
250 P(I,J)=0:PY(I,J)=0:PX(I,J)=0
260 NEXT I
270 '***** AVERAGE THE VALUES OF THE STREAM FUNCTION ON ****
280 '***** THE RIGHT AND LEFT BOUNDRIES *****
290 FOR I=1 TO 42 STEP 41
300 FOR J=3 TO 24
310 P(I,J)=(P(I,J-1)+P(I,J)+P(I,J+1))/3
320 NEXT J:NEXT I
330 FOR I=2 TO 10
340 FOR J=3 TO 24
350 P(I,J)=(P(I,J-2)+P(I,J)+P(I,J-1)+P(I,J+1)+P(I,J+2))/5
360 P(I+25,J)=(P(I+25,J-2)+P(I+25,J)+P(I+25,J-1)
+P(I+25,J+1)+P(I+25,J+2))/5
370 NEXT J
380 NEXT I
390 FOR I= 16 TO 26
400 P(I+2,7)= P(I+2,7)/8
410 P(I,8)= P(I,8)/12
420 'P(I,10)=P(I,10)/12
430 'P(I+2,11)= P(I+2,11)*(29-I)/12
440 NEXT I
450 FOR I=27 TO 32
460 P(I,8)= P(I,8)*(I-26)/12
470 P(I,9)= P(I,9)*(I-26)/12
480 P(I,7)= P(I,10)*(I-26)/3
490 NEXT I
500 FOR K=5 TO 19

```

```

510 PRINT USING"###.### ";P(20,23-K),P(21,23-K),P(22,23-K)
    ,P(23,23-K),P(24,23-K),P(25,23-K),P(26,23-K),P(27,23-K)
    ,P(28,23-K)
520 NEXT K
530 FOR I=3 TO 40
540 FOR J=3 TO 24
550 '**** CALCULATE THE 1st, 2nd, & 3rd DERIVATIVES *****
560 IF J= 9 AND I>10 AND I<27 THEN GOTO 590
570 PX(I,J)= (P(I+1,J) - P(I-1,J))/2/H
580 PY(I,J)= (P(I,J+1) - P(I,J-1))/2/H
590 PXX(I,J)= (P(I+1,J) - 2*P(I,J) + P(I-1,J))/H^2
600 PXXX(I,J)=(P(I+2,J)-2*P(I+1,J)+2*P(I-1,J)
    -P(I-2,J))/2/H^3
610 IF J= 9 AND I>10 AND I<27 THEN GOTO 710
620 PYY(I,J)= (P(I,J+1) - 2*P(I,J) + P(I,J-1))/H^2
630 IF J= 8 AND I>11 AND I<26 THEN GOTO 670
640 IF J=10 AND I>11 AND I<26 THEN GOTO 690
650 PYYY(I,J)=(P(I,J+2)-2*P(I,J+1)+2*P(I,J-1)
    -P(I,J-2))/2/H^3
660 GOTO 750
670 PYYY(I,J)= ( P(I,J+1)-3*P(I,J)+3*P(I,J-1)-P(I,J-2))/H^3
680 GOTO 750
690 PYYY(I,J)= (-P(I,J-1)+3*P(I,J)-3*P(I,J+1)+P(I,J+2))/H^3
700 GOTO 750
710 PYYT(I)=(P(I,J+2) - 2*P(I,J+1) + P(I,J))/H^2
720 PYYT(I)= (-P(I,J) + 3*P(I,J+1)-3*P(I,J+2)+P(I,J+3))/H^3
730 PYY(I,J)=(P(I,J-2) - 2*P(I,J-1) + P(I,J))/H^2
740 PYYY(I,J)= (P(I,J)- 3*P(I,J-1)+3*P(I,J-2)-P(I,J-3))/H^3
750 NEXT J
760 NEXT I
770 '***** CALCULATE THE CROSS DERIVATIVES *****
780 FOR I=3 TO 40
790 FOR J=3 TO 24
800 IF J= 9 AND I>10 AND I<27 THEN GOTO 850
810 IF J=10 THEN GOSUB 1300
820 PXXY(I,J)= (PXX(I,J+1)-PXX(I,J-1))/2/H
830 PYYX(I,J)= (PYY(I+1,J)-PYY(I-1,J))/2/H
840 PXXYY(I,J)= (PXX(I,J+1)-2*PXX(I,J)+PXX(I,J-1))/H^2
850 NEXT J
860 NEXT I
870 '***** ITERATIVE EQUATION FOR PSI *****
880 FOR J=3 TO 24
890 FOR I=3 TO 40
900 IF J= 9 AND I>10 AND I<27 THEN GOTO 1080
910 A=(PY(I,J)*(PYYX(I,J)+PXXX(I,J))-PX(I,J)*(PYYY(I,J)
    +PXXY(I,J)))*H^4/12/VIS
920 B=-H^4*PXXYY(I,J)/6
930 IF J= 8 AND I>11 AND I<26 THEN GOTO 980
940 IF J=10 AND I>11 AND I<26 THEN 1030
950 C=-.08333*(P(I-2,J)+P(I,J-2)+P(I+2,J)+P(I,J+2))
960 D=.3333*(P(I-1,J)+P(I,J-1)+P(I+1,J)+P(I,J+1))
970 GOTO 1070
980 A= A/12/7

```

```

990 B= B*12/7
1000 C= -(P(I,J-4) + P(I-2,J) + P(I+2,J))/7
1010 D= 4*(P(I-1,J) + P(I+1,J) + P(I,J-1) +P(I,J-3))/7
      - 6*P(I,J-2)/7
1020 GOTO 1070
1030 A= A*12/7
1040 B= B*12/7
1050 C= -(P(I,J+4) + P(I-2,J) + P(I+2,J))/7
1060 D= 4*(P(I-1,J) + P(I+1,J) + P(I,J+1) +P(I,J+3))/7
      - 6*P(I,J+2)/7
1070 P(I,J)=(A+B+C+D+90*P(I,J))/100
1080 NEXT I
1090 NEXT J
1100 J=2
1110 FOR I=2 TO 41
1120 P(I,J)=(P(I,J-1)+P(I,J+1))/2
1130 NEXT I
1140 J=J+23
1150 IF J>26 THEN 1160 ELSE 1110
1160 NIT=NIT+1
1170 IF NIT>NUM THEN 1180 ELSE 530
1180 FOR K=5 TO 19
1190 PRINT USING"####.### ";P(20,23-K),P(21,23-K),P(22,23-K)
      ,P(23,23-K),P(24,23-K),P(25,23-K),P(26,23-K),P(27,23-K)
      ,P(28,23-K)
1200 'LPRINT USING "###.### ";P(5,17-K),P(6,17-K),P( 7,17-K)
      ,P(8,17-K),P(9,17-K),P(10,17-K),P(11,17-K),P(12,17-K)
      ,P(13,17-K),P(14,17-K),P(15,17-K)
1210 NEXT K
1220 OPEN"O",#1,"FPLATE.DAT"
1230 FOR I=1 TO 42
1240 FOR J=1 TO 26
1250 PRINT#1,P(I,J)
1260 NEXT J
1270 NEXT I
1280 CLOSE
1290 END
1300 FOR L=11 TO 46
1310 PYY(L, 9)=PYVT(L)
1320 PYYY(L, 9)=PYVYT(L)
1330 NEXT L
1340 RETURN

```

LITERATURE CITED

- [1] Bird, R. B., W. E. Stewart, and E. N. Lightfoot, Transport Phenomena, pg. 504, John Wiley & Sons, New York (1960).
- [2] Boris, J. P., and D. L. Book. J. Comp. Phys. 20:397 (1976)
- [3] Canuto, C., Computing Methods in Applied Sciences and Engineering VI, pp. 335-351, Elsevier Science Pub. (N. Holland) (1984).
- [4] Canuto, C. and A. Quarteroni. Spectral Methods for Partial Differential Equations, pp. 55-78, SIAM Philadelphia (1984).
- [5] Deardorff, J. W. J. Fluid Mech., 41:453 (1970).
- [6] Dennis, S. C. R. and L. Quartapelle. J. Comp. Phys. 52:448 (1983).
- [7] Deville, M., P. Haldenwang, and G. Labrosse, Proc. 4th GAMM Conf. on Num. Meth. in Fluid Mech., pp. 64-76 (1982).
- [8] Finlayson, B. Nonlinear Analysis in Chemical Engineering, McGraw-Hill, New York (1980).
- [9] Gottlieb, D. and S. A. Orszag. Numerical Analysis of Spectral Methods: Theory and Applications, SIAM, Philadelphia (1977).
- [10] Gottlieb, D., M. Y. Hussaini and S. A. Orszag. Spectral Methods for Partial Differential Equations, pp. 1-54, SIAM, Philadelphia (1984a).
- [11] Gottlieb, D., L. Lustman and S. A. Orszag, SIAM, J. Sci. Stat. Comput. 2:296 (1981).
- [12] Gottlieb, D., L. Lustman and C. Streett. Spectral Methods for Partial Differential Equations, pp. 79-95, SIAM, Philadelphia (1984b).
- [13] Haidvogel, D. B., A. R. Robinson and E. E. Schulman. J. Comp. Phys. 34:1 (1980).
- [14] Haidvogel, D. B., and T. Zang, J. Comp. Phys. 30:167 (1979).
- [15] Hald, O. H. J. Comp. Phys. 40:305 (1981).
- [16] Haldenwang, P., G. Labrosse, and S. Abboudi, J. Comp. Phys. 55:115 (1984).
- [17] Hussaini, M. Y. and T. A. Zang. Spectral Methods for Partial Differential Equations, pp. 119-140, SIAM, Philadelphia (1984).

- [18] Jain, S. C. and K. S. Krishnan, Proc. Roy. Soc. (London) 2227A:141 (1955).
- [19] Kasahara, A., Computing Methods in Geophysical Mechanics 25:93 (1977).
- [20] Kleiser, L. Lecture Notes in Physics Vol. 170, pp. 280-285, Springer-Verlag, New York (1982).
- [21] Knudsen, J. G. and D. L. Katz, Fluid Dynamics and Heat Transfer, pp. 368-372, McGraw-Hill, New York (1958).
- [22] Ku, H. C. and D. Hatzivramidis, J. Comp. Phys., 56:495 (1984).
- [23] Ku, H. C. and D. Hatzivramidis, Comp & Fluids, 13:99 (1985).
- [24] Kumar, A. and K. S. Yajnik. J. Fluid Mech. 97:27 (1980).
- [25] Lamb, H. Hydrodynamics, Dover, New York (1945).
- [26] Lanczos, C. Applied Analysis, Prentics Hall Inc. Englewood Cliffs, N.J. (1956).
- [27] Leonard, A. and A. Wrey. Lecture Notes in Physics Vol. 170, pp. 335-342, Springer-Verlag, New York (1982).
- [28] Liepmann, H. W. Amer. Scientist, 67:221 (1979).
- [29] Maday, Y. and A. Quarteroni. SIAM J. Numer. Anal. 19:761 (1982).
- [30] Majda, A., J. McDonough and S. Osher. Math. Comp. 32:1041 (1978).
- [31] Malik, M. R., T. A. Zang and M. Y. Hussaini, J. Comp. Phys. 61:64 (1985).
- [32] Marcus, P. S., S. A. Orszag and A. T. Patera. Lecture Notes in Physics Vol. 170, pp. 371-376, Springer-Verlag (1982).
- [33] Mei, R. W. and A. Plotkin, AIAA 84-1616 (June 1984).
- [34] Metivet, B., and Y. Morchoisne, Proc. 4th GAMM Conf. on Num. Meth. in Fluid Mech., pp. 207-219 (1982).
- [35] Moin, P. Lecture Notes in Physics Vol. 170 pp. 55-76, Springer-Verlag, New York (1982).
- [36] Moin, P. and J. Kim. J. Comp. Phys. 35:381 (1980).
- [37] Orszag, S. A. Stud. Appl. Math. 50:293 (1971).
- [38] Orszag, S. A., Stud. Appl. Math. 51(3):253 (1972).

- [39] Orszag, S. A. Handbook of Turbulence, pp. 281-314, Plenum, New York (1977).
- [40] Orszag, S. A. J. Comp. Phys. 37:70 (1980).
- [41] Orszag, S. A. and L. C. Kells. J. Fluid Mech. 96:159 (1980).
- [42] Osher, S. Spectral Methods for Partial Differential Equations, pp. 209-216, SIAM, Philadelphia (1984).
- [43] Pasciak, J.E. Math. Comp. 35:1081 (1980).
- [44] Reddy, K. C., AIAA J. 21(8): 1208 (1983).
- [45] Roache, P. J., Computational Fluid Dynamics, Hermosa Pub., Albuquerque (1982).
- [46] Rudy, D. H. and J. C. Strikwerda. Comp. and Fluids, 9:327 (1981).
- [47] Sakell, L. AIAA J., 22:929 (1984).
- [48] Salas, M. D., T.A. Zang and M. Y. Hussaini. Lecture Notes in Physics Vol. 170, pp. 461-467, Springer-Verlag, New York (1982).
- [49] Schumann, U., Grotzbach, G., and L. Kleiser. Prediction Methods for Turbulent Flows, pp. 123-258, Hemisphere, Washington (1980).
- [50] Sharp, H. T., and W. L. Harris, J. Comp. Phys. 55:377 (1984).
- [51] Streett, C. L. and P. F. Bradley, Lecture Notes in Physics Vol. 218 pp. 536-540, Springer-Verlag, New York (1985).
- [52] Streett, C. L., T. A. Zang and M. Y. Hussaini. J. Comp. Phys. 57:43 (1985).
- [53] Tang, C., J. Comp. Phys. 32:80 (1979).
- [54] Taylor, T. D. Spectral Methods for Partial Differential Equations, pp. 257-267, SIAM, Philadelphia, (1984).
- [55] Taylor, T. D. and J. W. Murdock. Lecture Notes in Mathematics Vol. 771, pp. 519-537, Springer-Verlag, New York, (1980).
- [56] Taylor, T. D. and J. W. Murdock. Comp. & Fluids 9:255 (1981).
- [57] Taylor, T. D., R. B. Myers and J. H. Albert. Comp. & Fluids, 9:469 (1981).
- [58] Taylor, T. D., M. M. Nadworny and R. S. Hirsh, Lecture Notes in Physics Vol. 218, pp. 546-550, Springer-Verlag, New York (1985).

- [59] Tennekes, H. and J. L. Lumley. A First Course in Turbulence, MIT, Cambridge (1972).
- [60] Zang, T. A. and M. Y. Hussaini, Lecture Notes in Physics Vol. 218, pp. 603-607, Springer-Verlag, New York, (1985).
- [61] Zebib, A., J. Comp. Phys. 53:443 (1984).

AN EVALUATION OF THE APPLICABILITY OF PSEUDOSPECTRAL METHODS
TO PROBLEMS IN TRANSPORT PHENOMENA

by

GROVER TRAVIS JONES

B. S. Kansas State University, 1984

AN ABSTRACT OF A MASTER'S THESIS

submitted in partial fulfillment of the

requirements for the degree

MASTER OF SCIENCE

Department of Chemical Engineering

KANSAS STATE UNVIERSITY
Manhattan, Kansas

1986

ABSTRACT

The objective of this work was the evaluation of pseudospectral methods for their computational efficiency and applicability to problems in transport phenomena. This was accomplished by application of Chebyshev pseudospectral methods to problems from each major area of transport phenomena. The evaluation of the pseudospectral method was based upon comparison to the analytic solution, if available, or finite difference approximation otherwise. It was found that discontinuities in the solution domain can result in serious deviations from the correct solution; for example, the temperature discontinuity in thermal entrance length problems led to the propagation of error within the solution. Digital filtering was used successfully to damp out oscillatory behavior in all cases studied.